

## Theoretical and Experimental Studies of Adsorption Characteristics of Newly Synthesized Schiff Bases and their Evaluation as Corrosion Inhibitors for Mild Steel in 1 M HCl

Amel Ghames<sup>1,\*</sup>, Tahar Douadi<sup>1</sup>, Saifi Issaadi<sup>1</sup>, Lakhdar Sibous<sup>1</sup>, Khadija Ismaily Alaoui<sup>2</sup>, Mustapha Taleb<sup>2</sup> and Salah Chafaa<sup>1</sup>

<sup>1</sup> Laboratoire d'Electrochimie des Matériaux Moléculaires et Complexes, Département de Génie des Procèdes, Faculté de Technologie, Université FERHAT ABBAS - Sétif-1, 19000, Algérie.

<sup>2</sup> Laboratoire d'Ingénierie, d'Electrochimie, de Modélisation et d'Environnement (LIEME), Faculté des Sciences Dhar El Mahraz, Université Sidi Mohamed Ben Abdallah Fès, Maroc.

\*E-mail: [ghamesamel@yahoo.fr](mailto:ghamesamel@yahoo.fr)

Received: 13 December 2016 / Accepted: 20 April 2017 / Published: 12 May 2017

---

A new class of Schiff base compounds viz., 4,4'-bis(2,4-dihydroxybenzaldehyde) diphenylethanediiimine (L1) and 4,4'-bis(4-diethylaminosalicylaldehyde) diphenylethanediiimine (L2) have been synthesized and characterized by spectral techniques using Elemental analysis, FTIR, <sup>1</sup>H-NMR and mass spectrometry. The inhibition action on corrosion of the Schiff bases on mild steel in 1 M hydrochloric acid has been studied by the weight loss, potentiodynamic polarization and electrochemical impedance spectroscopy (EIS) methods were applied to study the corrosion at different concentrations of inhibitors. The inhibition efficiency has been compared with their parent amine from which the Schiff bases have been derived. The obtained results showed that L1 and L2 exhibited good inhibition on mild steel in HCl solution and the inhibition efficiency increased with increasing concentration, reaching a maximum inhibition efficiency of 95.33% and 94.18% designated respectively to L1 and L2 at 5x10<sup>-4</sup> M and decreased with increasing the temperature. Polarization study clearly suggested that these Schiff's bases act as mixed-type inhibitors with some cathodic predominance. The adsorption of L1 and L2 obeys Langmuir isotherm. SEM analyses revealed that inhibition occurs due to adsorption of molecules at metal/solution interface. Quantum chemical parameters were calculated using DFT method such as energy gaps support the good inhibiting performance of the two Schiff bases.

---

**Keywords:** Corrosion Inhibitors; Weight Loss; Electrochemical Measurements; Density Functional Theory; Fukui indices.

## 1. INTRODUCTION

Metal is a fundamental process of vital importance in economics and society. In order to prevent corrosion, the primary strategy adopted is to isolate the metal from corrosive media. It is a well-known fact that acids play crucial roles in our daily lives due to their excellent properties. These materials are used in many industrial processes such as acid cleaning, acid pickling, acid descaling, and oil well acidification [1- 3]. To prevent from acidic solutions aggression, the use of inhibitors is one of the most practical methods to control the corrosion of steel [4, 5]. In recent years different type organic compounds are used as inhibitors. The use of inhibitors is specific and must depend on the chemical composition of the solution, the nature of the metal surface, the temperature and the potential at the metal–solution interface. Nowadays, organic inhibitors compounds containing heteroatoms with electronic lone pair (N, O, S and P), or p systems, or conjugated bonds, or aromatic rings, are generally considered to be good corrosion inhibitors [6–9]. From this point of view, some reported the effect of Schiff base for steel [10–14], aluminum [15] and copper in acidic media [16, 17]. A great number of investigations revealed that Schiff bases show more inhibition efficiency than corresponding aldehyde and amines, and this may be due to the presence of a -C=N- group in the molecules [18]. For this reason it has recently been reported that a new potential class of corrosion inhibitors has recently emerged [19–22]. In the recent times, the uses of quantum chemical calculations in the estimation of reaction mechanisms and to analyze the experimental data have been extremely useful [23-27]. In this context, our contribution was to synthesize and evaluate, for the first time, the inhibitive effect of two newly heterocyclic Schiff bases [4,4'-bis(2,4-dihydroxybenzaldehyde) diphenylethanediiimine (L1) and 4,4'-bis(4-diethylaminosalicylaldehyde) diphenylethanediiimine (L2)] on mild steel X38 in hydrochloric acid using the electrochemical and gravimetric measurements. The experimental results were discussed with various activation and adsorption thermodynamic parameters. The passive film formed on the metal surface was characterized by EDX and SEM studies. Quantum chemical calculations were performed to investigate their relative corrosion inhibition performance from theoretical point of view. Several Quantum chemical properties and Mulliken atomic charges are hereby studied using density functional theory (DFT) at B3LYP/6-31G (d, p) level. Local reactive sites of the present molecules have been analyzed through Fukui indices. This study could provide important information discover new inhibitors with better efficacy.

## 2. EXPERIMENTAL

### 2.1. Inhibitors synthesis

The heterocyclic Schiff bases; 4,4'-bis(2,4-dihydroxybenzaldehyde) diphenylethanediiimine (L1) and 4,4'-bis(4-diéthylaminosalicylaldehyde)diphényléthanediiimine (L2) shown in Fig.1 were synthesized in our laboratory, and were prepared according to the method described in the literature [28], by a simple condensation reaction between 0.2 g (1 mmol) of 4,4'-diaminodiphenylethane (C<sub>14</sub>H<sub>16</sub>N<sub>2</sub>, Mol. Wt. 212.29) and corresponding aldehydes: 0.18 g (2 mmol) 2,4-dihydroxy

benzaldehyde ( $C_7H_6O_3$ , Mol. Wt. 138.12) for L1, or with 0.18 g (2 mmol) 4-diethylaminosalicylaldehyde ( $C_{11}H_{15}NO_2$ , Mol. Wt. 193.25) in case of L2. The reactions were carried out in 20 mL of absolute ethanol. The mixture of both solutions was refluxed for 3 h with stirring, and then cooled to room temperature. The solution was concentrated using the rotary evaporator. The final products were collected by filtration, washed with ethanol and purified by recrystallizing from EtOH-THF (3/7, v/v) mixture and dried in air. The molecular structure and spectroscopic properties of the synthesized compounds L1 and L2 were confirmed using  $^1H$  NMR, IR spectroscopy and elemental analysis. The Schiff bases under investigation were subjected to (C, H and N) elemental analysis which was performed using the "Service d'Analyse du C.N.R.S de l'I.C.S.N., Gif sur Yvette (France)". The mass spectrum was determined using EI technique conditions at 70 eV and recorded on an MS-5988 GC-MS Hewlett-Packard instrument. Melting point was determined on "Kofler bank Melting point Apparatus". Infrared spectra were recorded on Perkin-Elmer 1000 series FTIR spectrophotometer, using KBr disks. UV-Vis absorption spectra were recorded on a UNICAM UV300 spectrophotometer in DMF solutions, using 1 cm quartz cuvettes.  $^1H$ -NMR spectra were measured on a model Bruker Advance 300 (MHz) using  $DMSO-D_6$  as solvent; the chemical shifts are reported in  $\delta$ (ppm) unit downfield internal reference (TMS).

4,4'-bis(2,4-dihydroxybenzaldehyde) diphenylethanediimine(L1) [ $C_{28}H_{24}N_2O_4$ , Mol.Wt.452.67]: Yield: 78.53%. m.p.= 220 °C ; Anal.Calc. %: C, 74.29; H, 5.34; N, 6.18; O, 14.08. Found %: C, 74.33; H, 5.34; N, 6.19; O, 14.15.  $^1H$  RMN ( $DMSO-d_6$ ),  $\delta$  (ppm), 300 MHz): 6.4(2d, 4H, HC=CH), 7.0 (m, 3H, Ar-H), 7.8 (s, 1H, HC=N), 10.25 and 13.6 (2s, 2H, 2xOH).  $\nu_{max}$  (KBr): C=N, 1627.23  $cm^{-1}$ ;  $\lambda_{max}$  = 348 nm ( $\epsilon = 91.034 \times 10^2 L mol^{-1} cm^{-1}$ )  $k_{max}$  (nm) [ $\epsilon_{max}$  (dm<sup>3</sup> mol<sup>-1</sup> cm<sup>-1</sup>)] (acetonitrile);  $M^+$ :453.2.

4,4'-bis(4-diéthylaminosalicylaldehyde) diphenyléthanediimine (L2) [ $C_{36}H_{42}N_4O_2$ , Mol.Wt. 562,74]: Yield: 63.63%. m.p.> 260 °C; Anal.Calc. %: C, 76.8; H, 7.52; N, 9.95; O, 5.73. Found %: C, 76.86; H, 7.47; N, 9.96; O, 5.69.  $^1H$  RMN ( $DMSO-d_6$ ),  $\delta$  (ppm), 300 MHz): 2.08 (t, 6H, 2CH<sub>3</sub>), 4.2 (q, 4H, 2CH<sub>2</sub>), 6.5- 7.45 (m, 5H, Ar-H), 7.69(s, 1H, CH=N), 13.2 (s, 1H, Ar-OH).  $\nu_{max}$  (KBr): C=N, 1626.65  $cm^{-1}$ ;  $\lambda_{max}$  = 386 nm ( $\epsilon = 31.347 \times 10^2 L mol^{-1} cm^{-1}$ )  $k_{max}$  (nm) [ $\epsilon_{max}$  (dm<sup>3</sup> mol<sup>-1</sup> cm<sup>-1</sup>)] (acetonitrile);  $M^+$ :563.4.

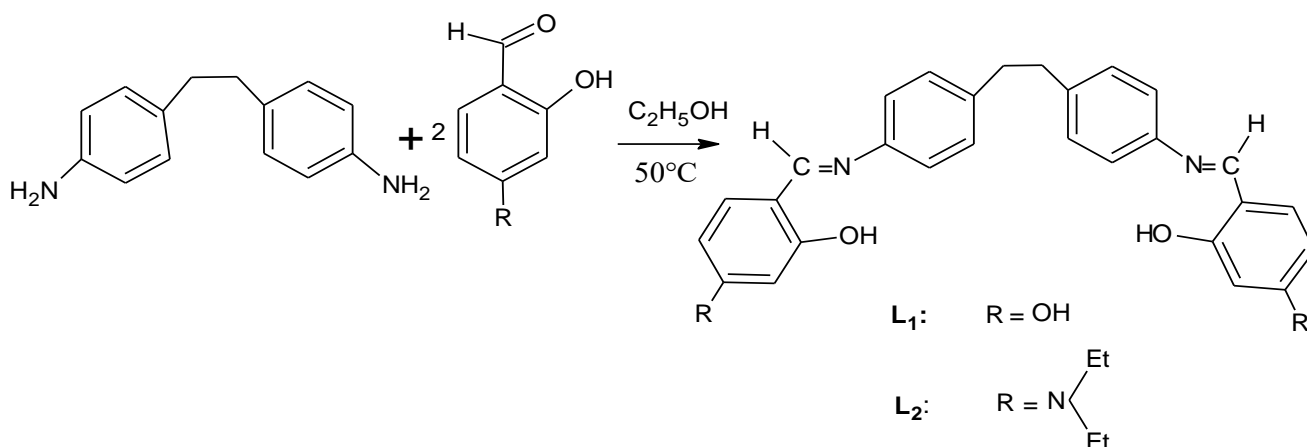


**Figure 1.** Synthesis procedure and general structures of investigated Schiff bases.

## 2.2. Materials preparation

All commercial reagents and solvents were analytical grade (AR), The chemicals used included 4,4'-diaminodiphenylethane, 2,4-dihydroxy benzaldehyde and 4-diethylaminosalicylaldehyde were purchased from Sigma-Aldrich (France) and used as received without further purification. Prior to all measurements, the mild steel specimens used in the present study had composition (wt %) Fe 99.21 %, C 0.21%, Si 0.38%, P 0.09%, Mn 0.05%, S 0.05%, Al 0.01%, were used for electrochemical and gravimetric studies, were mechanically abraded using emery paper (400, 600, 800, 1000 and 1200 mesh/in grade). The surface and thickness of the test electrode were measured and washed with distilled water, cleaned with acetone and finally dried in hot air. The test solution 1 M HCl prepared from analytical grade reagent (37% HCl) and double-distilled water. The working concentrations of inhibitors varied from  $1.0 \times 10^{-5}$  M to  $5.0 \times 10^{-4}$  M in 1 M HCl. Doubly distilled water was used in the preparation of the various concentrations of test solutions.

## 2.3. Measurements

Gravimetric and electrochemical techniques were used to evaluate the inhibition efficiency of the investigated Schiff bases L1 and L2.

### 2.3.1. Weight loss method

Weight loss experiments were carried out as described [17- 29]. Mild steel specimens having the dimension of  $2 \times 1 \times 0.5$  cm. Gravimetric tests were performed by weighing cleaned and dried MS specimens before and after immersion in test solution of 1 M HCl for 6 h at different concentrations ( $1 \times 10^{-5}$  M to  $5 \times 10^{-4}$  M) of the studied Schiff bases at 25°C. The temperature was controlled by an aqueous thermostat bath. The experiments were carried out in duplicate and average values were obtained. The weight loss allowed the calculation of the mean corrosion rate in  $\text{mg cm}^{-2} \text{h}^{-1}$ . The corrosion rate ( $C_R$ ), the degree of surface coverage ( $\theta$ ) and the inhibition efficiency  $IE$  (%) were calculated at different concentration [30- 32].

$$C_R = \frac{W}{At} \quad (1)$$

$$\theta = \frac{C_R - C_{R(i)}}{C_R} \quad (2)$$

$$IE_{WL} \% = \frac{C_R - C_{R(i)}}{C_R} \times 100 \quad (3)$$

Where,  $W$  is the weight loss of specimens (mg),  $A$  is the area of the specimen ( $\text{cm}^2$ ) and  $t$  is the immersion time ( $h$ ).  $C_R$  and  $C_{R(i)}$  are the corrosion rates in the absence and presence of the inhibitors L1 and L2 respectively

### 2.3.2. Electrochemical measurements

Polarization study was performed in a conventional three electrode cylindrical Pyrex glass cell connected with a Potentiostat model Voltalab PGZ100 and piloted by Voltmaster 4. The mild steel was used as the working electrode, a platinum electrode was used as the counter electrode and the reference electrode was a saturated calomel electrode (SCE). The surface area exposed to the electrolyte is  $1 \text{ cm}^2$  and the working electrode was immersed in the test solution for 30 minutes and to a establish steady-state (open circuit) potential ( $OCP$ ) corresponding to the corrosion potential ( $E_{corr}$ ) of the working electrode was obtained. After measuring the  $E_{ocp}$ , the polarization measurements were performed. The potentiodynamic curves were recorded by sweeping the electrode potential from  $-700$  to  $-200 \text{ mV/SCE}$  at a constant sweep rate  $1 \text{ mV/s}$ . The corrosion inhibition efficiency was calculated from the corrosion current values determined from the Tafel extrapolation method using the experimental relation:

$$IE(\%) = \frac{i_{corr}^0 - i_{corr}}{i_{corr}^0} \times 100 \quad (4)$$

Where  $i_{corr}^0$  and  $i_{corr}$  are the corrosion current densities in the uninhibited and inhibited solutions, respectively. EIS measurements were performed using PGZ 100, with a small amplitude AC signal  $10 \text{ mV}$ , at frequencies between  $100 \text{ KHz}$  to  $10 \text{ mHz}$  with 10 points per decade, at open circuit potential ( $E_{corr}$ ). After the immersion, the impedance diagrams are given in the Nyquist representation and the impedance data were analyzed and fitted with ZView 2.80, equivalent circuit software. The use of the non-linear least squares fit allowed us to give the intersections with the x-axis and this was done by fitting the best semicircle through the data points in the Nyquist plot. The charge transfer resistance ( $R_{ct}$ ), double layer capacitance ( $C_{dl}$ ) and other parameters were calculated. The inhibition efficiency  $IE(\%)$  from impedance measurements was calculated by the following expression [33].

$$IE(\%) = \frac{R_{ct} - R_{ct}^0}{R_{ct}} \times 100 \quad (5)$$

Where,  $R_{ct}$  and  $R_{ct}^0$  are charge transfer resistance without and with inhibitors, respectively.

### 2.3.4. Surface morphology

The surface examinations of mild steel samples with and without optimum concentration of inhibitors were immersed in  $1 \text{ M HCl}$  solution for 6 hours. Subsequently, the mild steel specimens were removed; washed and dried. FEI quanta 200 scanning electron microscope was used for this

study. All Micrographs of the corroded specimens were enlarged to 200 in order to present a constant view.

### 2.3.5. Quantum chemical calculations

Quantum chemical method was performed to explore the correlation between molecular properties of the studied inhibitors in line with its corresponding inhibition efficiency. From a computational point of view DFT (Density Functional Theory) methods have become popular from the last few decades for their accuracy in respective calculation in lesser time with a much less investment. In this present study DFT calculations were performed using the Gaussian 03 programme package [34]. Complete geometry optimization of the molecules was carried out by density functional theory (DFT) level with the non-local hybrid density functional B3LYP/6-31G (d, p) basis set [35-37]. This approach is widely used in the analysis of the characteristics of the corrosion process and allows obtaining favorable geometries for a wide variety of systems. Some molecular descriptors were evaluated from the obtained optimized molecular structure: HOMO and LUMO energy values, the energy band gap ( $\Delta E_{gap}$ ), molecular dipole moment ( $\mu$ ), global hardness ( $\eta$ ), softness ( $\sigma$ ), electrophilicity index ( $\omega$ ), Total energy (TE) and the Mulliken charges, the absolute electronegativity ( $\chi$ ) and the number of transferred electrons ( $\Delta N$ ), were calculated using DFT and correlated with inhibition efficiencies. The local reactivity was analyzed through Fukui function.

## 3. RESULTS AND DISCUSSION

### 3.1. Mass spectroscopy

The electron impact mass spectra of both Schiff bases are investigated and recorded at 70eV of electron energy. The spectra are characterized by moderate to high relative intensity molecular ion peaks. The mass spectrum of the studied products using electron impact (EI) conditions gave the parent ion peaks  $M^+$  at  $m/z$  453.2 (R.I = 100%, base peak) and 563.4 (R.I = 100%, base peak) which are close to the calculated formulas  $m/z$  452.67 and  $m/z$  562.74. These values are assigned, respectively, to the species L1 and L2, supporting the structures of the Schiff bases. It is observed that the abundance of the molecular ions depends mainly on the structures of L1 and L2. Other molecular ion peaks in the range, i.e. 97.8, 120.2, 156.3, 183.8, 213 and 333u can be attributed to L1 and L2, i.e. 98, 157, 194, 229.8, 388.2 and 422.2 are designated for L2. However, the abundance of the ion peaks from the range 1–100 % may be attributed to the fragmentation of the Schiff bases obtained from the rupture of different bonds inside the molecule. It is apparent that, the molecular ion peaks are in good agreement with their proposed empirical formula.

## 3.2. Weight loss measurements

## 3.2.1. Influence of concentration

**Table 1.** Inhibition efficiencies for various concentrations of L1 and L2 for corrosion of MS specimens immersed in 1M HCl for 6 h by weight loss measurements.

<i>Inhibitor</i>	<i>Concentration (M)</i>	<i>Weight loss (mg cm<sup>-2</sup>h<sup>-1</sup>)</i>	<i>IE<sub>WL</sub> (%)</i>	<i>θ</i>
1M HCl(Blank)	-	0.9596	-	-
4,4'-diaminodiphenylethane (M1)	1×10 <sup>-5</sup>	0.6675	30.43	0.30
	5×10 <sup>-5</sup>	0.6097	36.46	0.36
	1×10 <sup>-4</sup>	0.5366	44.08	0.44
	5×10 <sup>-4</sup>	0.3218	66.46	0.66
4,4'-bis(2,4-dihydroxybenzaldehyde) diphenylethanedimine (L1)	1×10 <sup>-5</sup>	0.0689	92.81	0.92
	5×10 <sup>-5</sup>	0.0564	94.12	0.94
	1×10 <sup>-4</sup>	0.0462	95.18	0.95
	5×10 <sup>-4</sup>	0.0245	97.44	0.97
4,4'-bis (4-diethylaminosalicylaldehyde) diphenylethane (L2)	1×10 <sup>-5</sup>	0.0770	91.97	0.91
	5×10 <sup>-5</sup>	0.0716	92.53	0.92
	1×10 <sup>-4</sup>	0.0625	93.48	0.93
	5×10 <sup>-4</sup>	0.0413	95.57	0.95

Gravimetric measurements were performed in order to determine the corrosion rate and the percent of the inhibition efficiency. This physical measurement will furnish direct response on how the corrosion environments affect the samples and also show the average corrosion rate during the experiments. Table 1 shows the values of inhibition efficiency and corrosion rates of the mild steel with and without the addition of different inhibitor concentrations determined after 6h at room temperature. The results show that both, L1 and L2, act effectively as corrosion inhibitors.

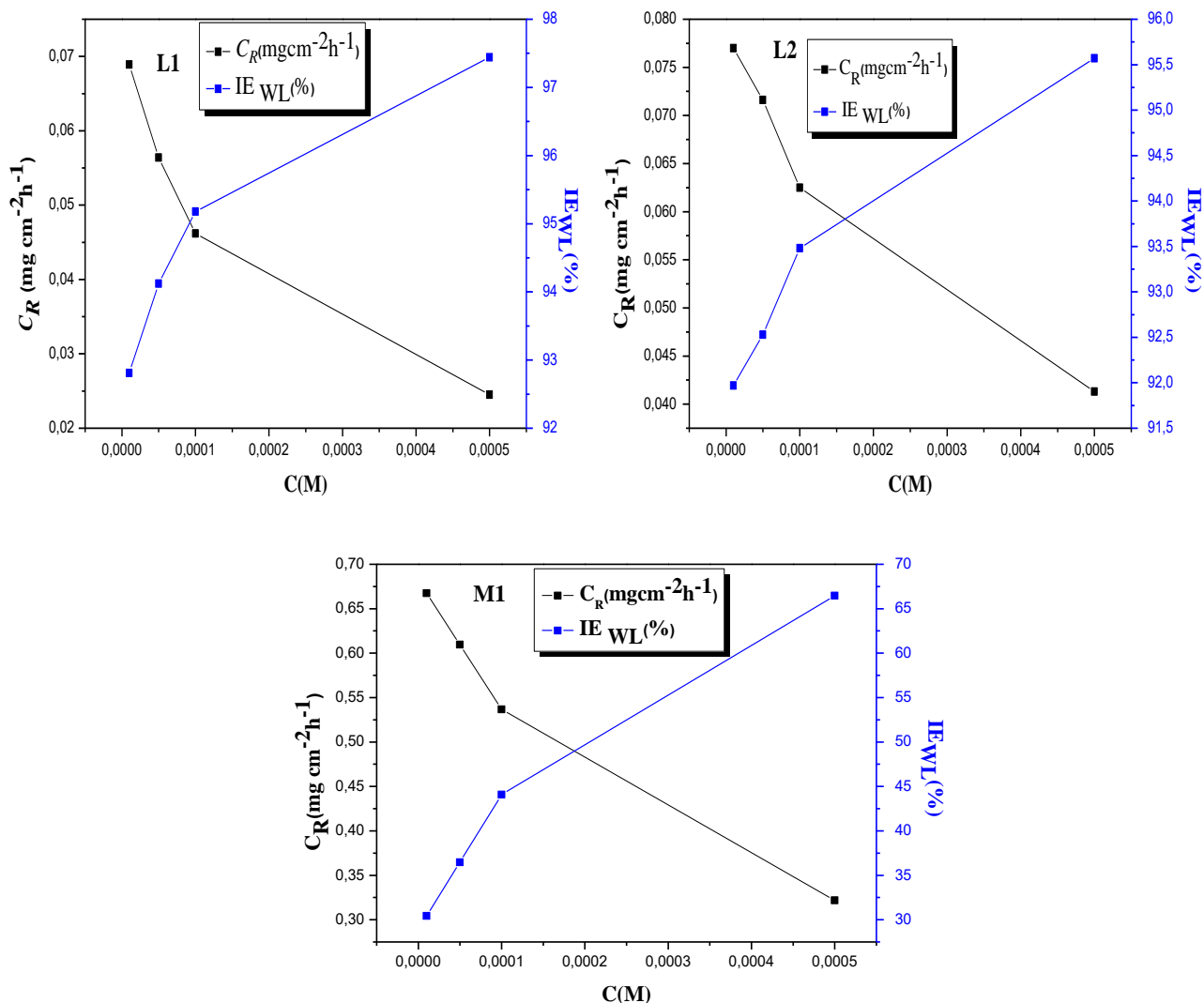


**Figure 2.** Relationship between the inhibition efficiency (IE%) and corrosion rates ( $C_R$ ) vs. Concentrations ( $C$ ) for steel after 6 h immersion in 1 M HCl of L1, L2 and M1.

To compare the inhibition efficiency of Schiff base and parent amine, weight loss measurements of MS specimens in HCl containing various concentrations of the Schiff bases L1 and L2 and the parent amine M1 were carried out at 25 °C. It was observed that these compounds M1, L1 and L2 decrease the value of corrosion rate of mild steel with the increasing in the concentration of the compounds tested (Fig.2). This can result from the fact that adsorption and surface coverage have increased with increasing concentrations. The corrosion inhibition values which were obtained are shown in table 1. It is evident to note that inhibition performance increases with increasing inhibitor concentrations and inhibition efficiency of the Schiff bases L1 and L2 was marked higher than the corresponding parent amine M1, for the studied concentrations (Fig.3). The high inhibition efficiency was obtained at  $5 \times 10^{-4}$  M for M1, L1 and L2 attains respectively 66.46%, 97.44%, 95.57%, is attributed to the presence of several heteroatoms in the form of polar functional groups. From weight loss measurements, it can be deduced that the inhibition efficiency of the three tested compounds follows the order: L1 > L2 > M1. The presence of  $-C=N-$  group, which is not present in the parent

amine, is responsible for the higher inhibition efficiency of the Schiff base than parent amine. This investigation, clearly establishes the role of azomethine linkage (C=N), the OH group present in the Schiff base which actively participate in the corrosion inhibition mechanism [38-40]. The oxygen and the nitrogen atoms of the inhibitors L1 and L2 are probably the active adsorption centers on the surface of mild steel.

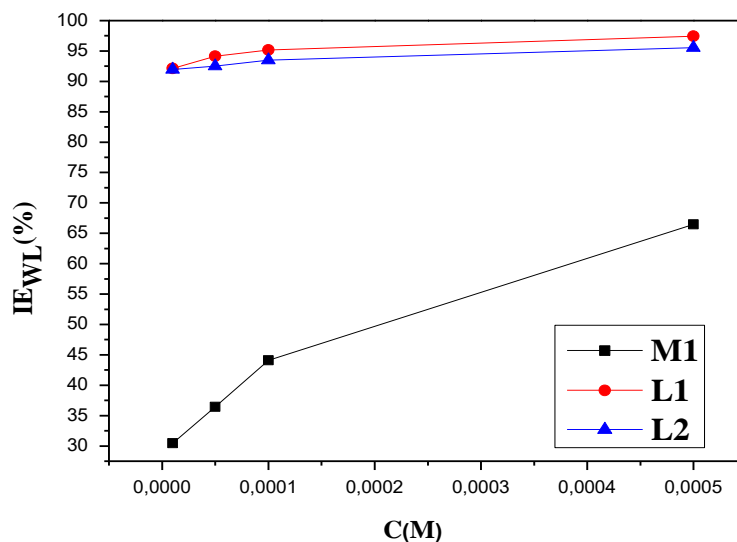


**Figure 3.** Comparison of inhibition efficiency of Schiff base and parent amine (M1) obtained for different concentrations in 1M HCl.

### 3.3. Thermodynamic activation parameters

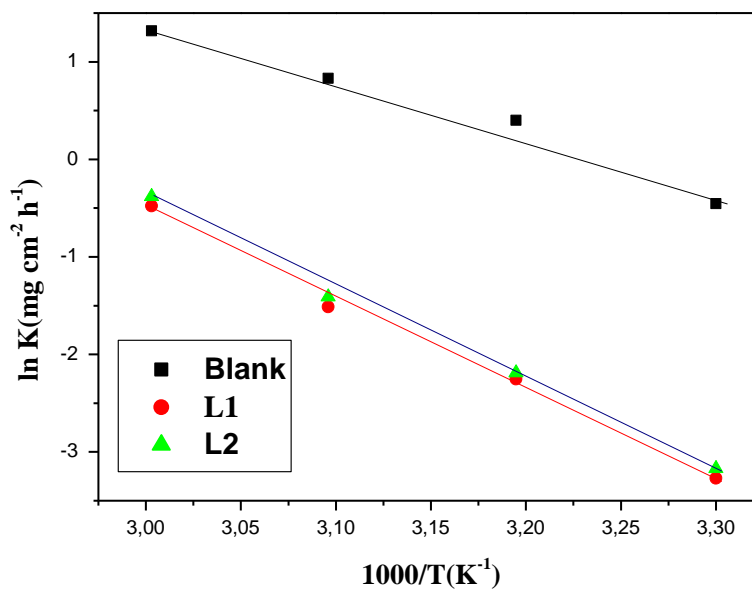
In order to collect more information about the activation parameters of the Schiff base inhibitors for mild steel in 1 M HCl solution, Weight loss measurements were carried out at optimum concentration of L1 and L2 in a temperature range of 30 to 60 °C. The Arrhenius Eq. (6) represents the effect of temperature on the corrosion inhibition efficiency of the studied Schiff bases, indicating the natural logarithm of corrosion rate (log C<sub>R</sub>) as a linear function of 1/T as shown in Fig.4.

$$K = A \exp\left(\frac{-E_a}{RT}\right) \quad (6)$$

Where *K* is the rate of metal dissolution, *A* the pre-exponential factor, *E<sub>a</sub>* the activation energy of the metal dissolution reaction, *T* the absolute temperature and *R* is the gas constant. Values of the activation corrosion energy are obtained from the slope values of Arrhenius plots shown in Fig. 4.

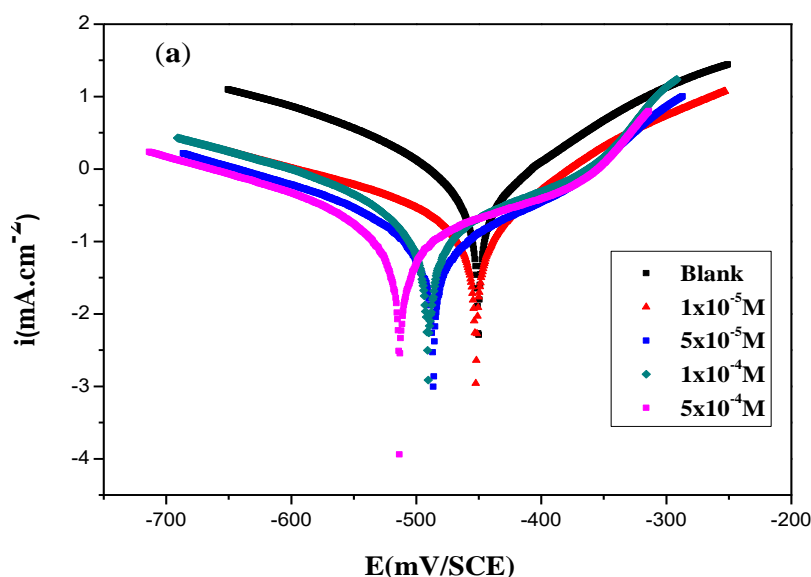
All the linear regression coefficients are close to unity, the kinetic model is used to elucidate the corrosion of the steel in hydrochloric acid. The calculated values of *E<sub>a</sub>* are found as 37.801, 68.895 and 62.031 kJ mol<sup>-1</sup>, for 1M HCl, L1 and L2 respectively. The results showed that the values of *E<sub>a</sub>* in the presence of inhibitors are higher than obtained in the blank solution. This indicates that the

corrosion rate of the mild steel is controlled by the activation [41, 42]. It is well known that the inhibition efficiency is related to the effect of temperature and correlates with the activation energy values of the corrosion process in the absence and presence of the Schiff bases, which can also provide additional evidence regarding the mechanism of action of inhibition [43]. According to other authors [44], the higher value of  $E_a$  is interpreted as an indication for an electrostatic character of the inhibitor's adsorption.



**Figure 4.** Arrhenius plots to calculate the activation energy of corrosion of MS in the absence and presence of  $5 \times 10^{-4}$  M of the studied inhibitors.

### 3.4. Potentiodynamic polarization studies



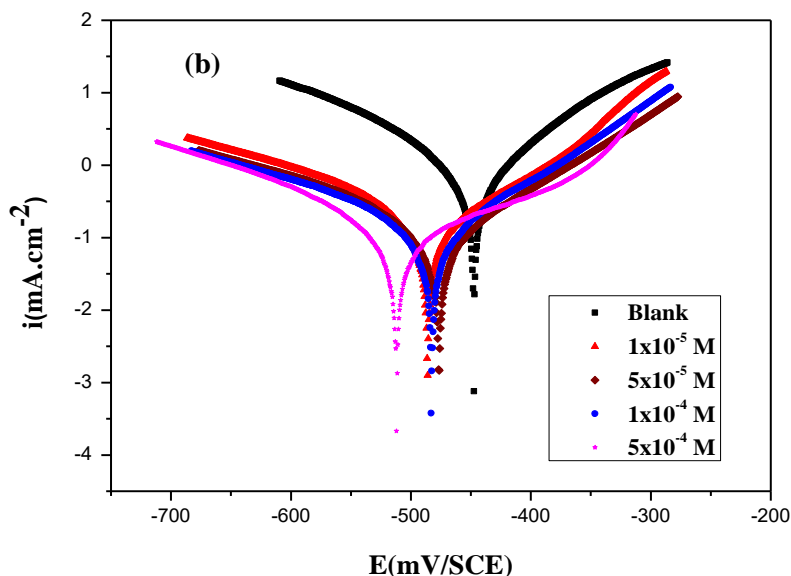


**Figure 5.** Potentiodynamic polarization curves for mild steel in 1 M HCl in the presence and absence of different concentrations of (a) L1 and (b) L2.

Polarization curves were obtained for mild steel in HCl solution with and without inhibitors. Tafel lines were obtained in various concentrations of L1 and L2 solutions are shown in Fig.5. The electrochemical parameters such as current density ( $I_{corr}$ ), corrosion potential ( $E_{corr}$ ), Tafel constants ( $b_a$  and  $b_c$ ) were calculated by extrapolating the Tafel slope, surface coverage ( $\theta$ ) and inhibition efficiency are given in Table 2.

**Table 2.** Electrochemical parameters calculated from Tafel extrapolation measurements in 1M HCl solution with and without inhibitors concentrations.

Inhibitor	C (M)	$E_{corr}$ (mV/SCE)	$b_a$ (mV/dec)	$-b_c$ (mV/dec)	Tafel data $I_{corr}(\mu A/cm^2)$	$R_p$ ( $\Omega cm^2$ )	$I\bar{E}_p$ (%)	$\theta$
1M HCl(Blank)	-	-450.1	160.4	225.6	1626.2	18.47	-	-
4,4'-bis(2,4-dihydroxybenzaldehyde) diphenylethanediiimine (L1)	$1 \times 10^{-5}$	-452.3	96.7	183.5	178,3	140.43	89.03	0.89
	$5 \times 10^{-5}$	-486.5	146.9	101.7	117,58	214.13	92.76	0.92
	$1 \times 10^{-4}$	-490.5	131.4	108.4	82.93	239.51	94.89	0.94
	$5 \times 10^{-4}$	-513.1	163.1	106.3	75.81	266.17	95.33	0.95
4,4'-bis(4-diethylaminosalicylaldehyde) diphenylethanediiimine(L2)	$1 \times 10^{-5}$	-485.8	153.5	172.6	210.51	160.83	87.05	0.87
	$5 \times 10^{-5}$	-476.2	128.8	161.8	129.79	218.16	92.01	0.92
	$1 \times 10^{-4}$	-482.6	119.7	158.7	124.34	243.08	92.35	0.92
	$5 \times 10^{-4}$	-511.9	189.9	119.1	94.56	243.20	94.18	0.94

The examination of the results listed in Table 2, showed that the density of the corrosion current decreases by increasing the concentrations in the presence of L1 and L2; significantly

indicating the formation of a protective film by inhibitory molecules and therefore inhibition occurs [45]. This demonstrates the effective inhibitive nature of the Schiff base molecules [46]. Moreover, it is seen that the corrosion current density ( $i_{corr}$ ) became lower with inhibitors than acid solution, which exhibited a maximum inhibition efficiency of 95.33% and 94.18% designated respectively to L1 and L2. The cathodic Tafel curves in Fig. 5 give rise to parallel lines show that the additions of the Schiff base inhibitors do not modify the hydrogen evolution mechanism and the reduction of hydrogen ions on the mild steel surface takes place mainly through a charge transfer mechanism [47]. The adsorbed inhibitors molecules only block the active sites of hydrogen evolution on the metal surface. However, for potential higher than -300 mV (SCE), the presence of Schiff base molecules did not change the current-vs.-potential characteristics and the inhibition efficiency decreases in anodic domain (Fig. 5). This potential can be defined as the desorption potential. The phenomenon may be explained by the equality of the rate of adsorption of inhibitor and that of the metal oxidation leading to a desorption of the inhibitor molecules from the electrode surface [48]. If the change in corrosion potential is greater than  $\pm 85$  mV with respect to the corrosion potential of the blank solution, the inhibitor can be considered as anodic or cathodic type [49]. Concerning the present case, the potential shifts in the presence of L1 and L2 to more negative value and are less than 85 mV, indicating that the investigated inhibitors act as mixed-type inhibitor with slight predominant cathodic effectiveness [50, 51]. Schiff base molecules exhibit the best inhibition efficiency, probably because of the excess nitrogen atoms and the presence of aromatic ring in the molecules, which can increase the adsorption of molecules on the surface. The results obtained from the polarization in acidic solution were in good agreement with those obtained from the weight loss.

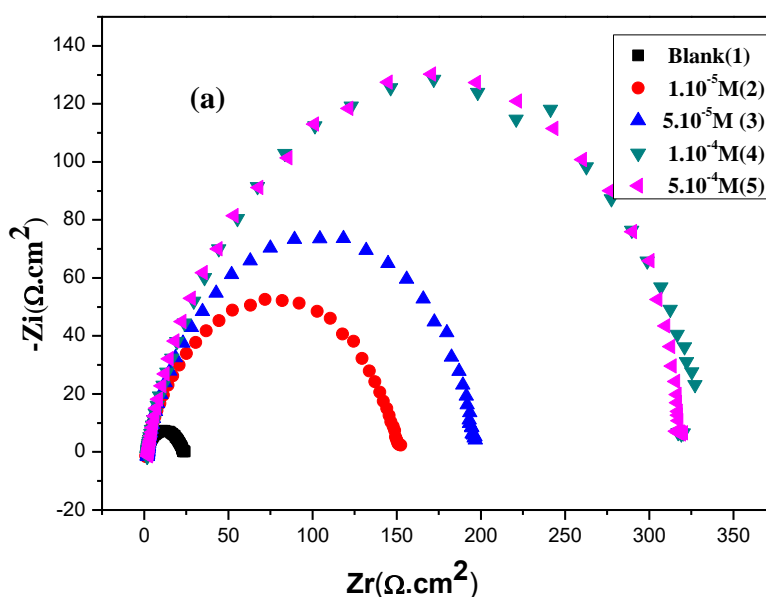
### 3.5. Electrochemical impedance spectroscopy (EIS) measurements

The experimental results can be interpreted in terms of the equivalent circuit of the electrical double layer, which used previously to model the steel-acid interface [12]. The corrosion response of the mild steel in 1M HCl solution with and without inhibitors was also investigated by electrochemical impedance spectroscopy (EIS) measurements. Fig.6. represents the Nyquist plots of MS specimens in HCl. It is evident from the plots that the impedance response of metal specimens shows a marked difference in the presence and absence of the inhibitors L1 and L2. From a visualization of the Nyquist plots, the diameter of the half-circle capacitive loop increases in the presence of an increasing concentration of inhibitor. The increasing diameter of capacitive loop indicated the inhibition of corrosion of mild steel, which indicates the adsorption of inhibitors on the metal surface. The capacitance loop intersects the real axis at higher and lower frequencies. At high frequency end, the intercept corresponds to the solution resistance ( $R_s$ ) and at lower frequency end corresponds to the sum of  $R_s$  and charge transfer resistance ( $R_{ct}$ ). The technical behavior can be well explained by pure electrical models that can verify and allow calculating numerical values corresponding to the physical and chemical properties of the electrochemical system under examination. EIS spectra were analyzed using the equivalent circuit in Fig. 7. It included ( $R_s$ ) solution resistance, in series with the parallel

combination of the double-layer capacitance ( $C_{dl}$ ) and a charge transfer- resistance ( $R_{ct}$ ) [52, 53]. The value of double layer capacitance ( $C_{dl}$ ) was calculated by using the following equation:

$$C_{dl} = \frac{1}{2\pi f_{max}} \times \frac{1}{R_{ct}} \quad (7)$$

In the above relation  $f_{max}$  presents the frequency at which the imaginary part of the impedance reaches a maximum. The calculated impedance parameters such as  $R_{ct}$ ,  $C_{dl}$  and  $IE(\%)$  are listed in Table 3. From the plots, it is clear that there is a significant change in the steel impedance response of the uninhibited solution and the corrosive solution. This indicates that the impedance of the inhibited substrate increased with increasing inhibitor concentration [54, 55]. From results obtained, the values of  $R_{ct}$  increase, the  $C_{dl}$  values also decrease with increasing concentration of inhibitors, the increase in the quantum of adsorption of the surface-inhibiting molecules is the result of a decrease in the local dielectric constant and / or an increase in the thickness of the electrical double layer. This implies that the change in  $C_{dl}$  values was provided because of the gradual replacement of water molecule from the steel surface by the inhibitor molecule thereby reducing the active sites of corrosion [56]. The inhibition efficiency increases with increasing inhibitor concentration due to more and more coverage of mild steel surface with the inhibitor concentrations. The high values of the inhibition efficiency are 93.70%, 92.64% for respectively L1 and L2 at  $5 \times 10^{-4}$  M. Variation in the  $IE \%$  might be due to the substituents, molecular mass and molecular sizes of the inhibitors [57]. It is clear that there is conformity between the impedance graph measured and that computed by the equivalent circuit model used. Fig. 7 is an equivalent circuit generally used to represent the corrosion process on the mild steel in hydrochloric acid.



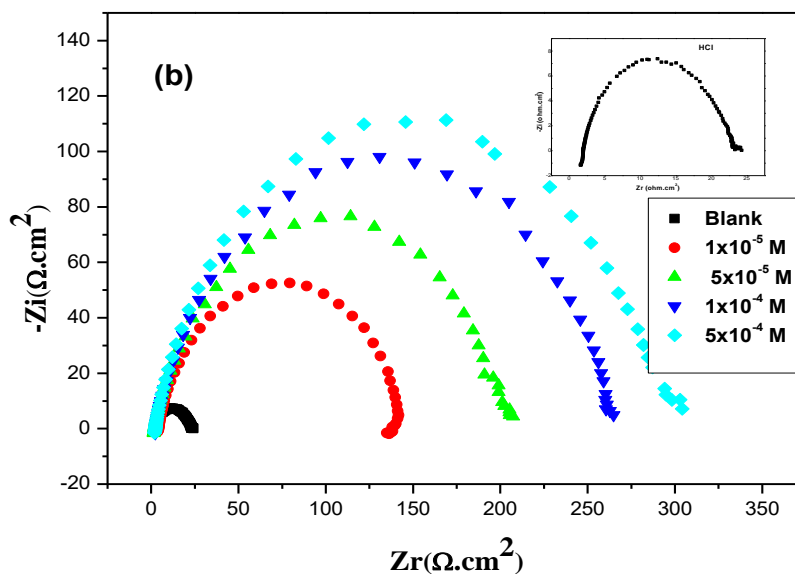


**Figure 6.** Nyquist plot for mild steel in 1.0 M HCl in the presence and absence of different concentrations of (a) L1 and (b) L2.

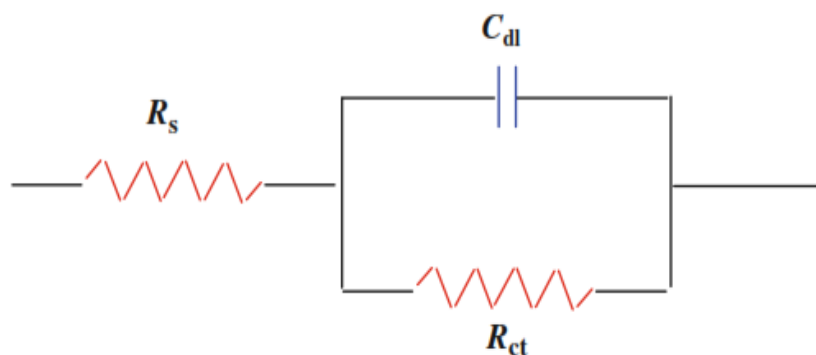


**Figure 7.** Equivalent circuit model for impedance analysis.

Moreover, the Bode and phase angle plots for mild steel in 1 M HCl with and without of inhibitors L1 and L2 were plotted using the same experimental data in the Nyquist format (Fig. 8). The high-frequency intercept with the real axis in Bode plot is attributed to the charge transfer reaction and time constant of the electric double layer and to the surface non-homogeneity of structural or interfacial origin, such as those found in adsorption processes. The low-frequency inductive loop may be attributed to the relaxation of adsorbed compound on electrode surface [58]. The Fig. 8a shows the impedance plots at the low frequency move to higher absolute values as the inhibitor concentration increases, suggesting the great resistance of the adsorbed layer which is related to the adsorption of azomethine compounds on the mild steel surface in HCl [59]. The curves of the small phase angle (Fig. 8b) is ascribed to some physical nature of surface *i.e.*, inhomogeneity, roughness and active site of surface of the mild steel resulting from the attack of corrosive medium. The continuous increase in the phase angle shift is corresponding to the development of the surface coverage by the inhibitor molecules [60]. Excellent fit with this model was obtained for all experimental data.

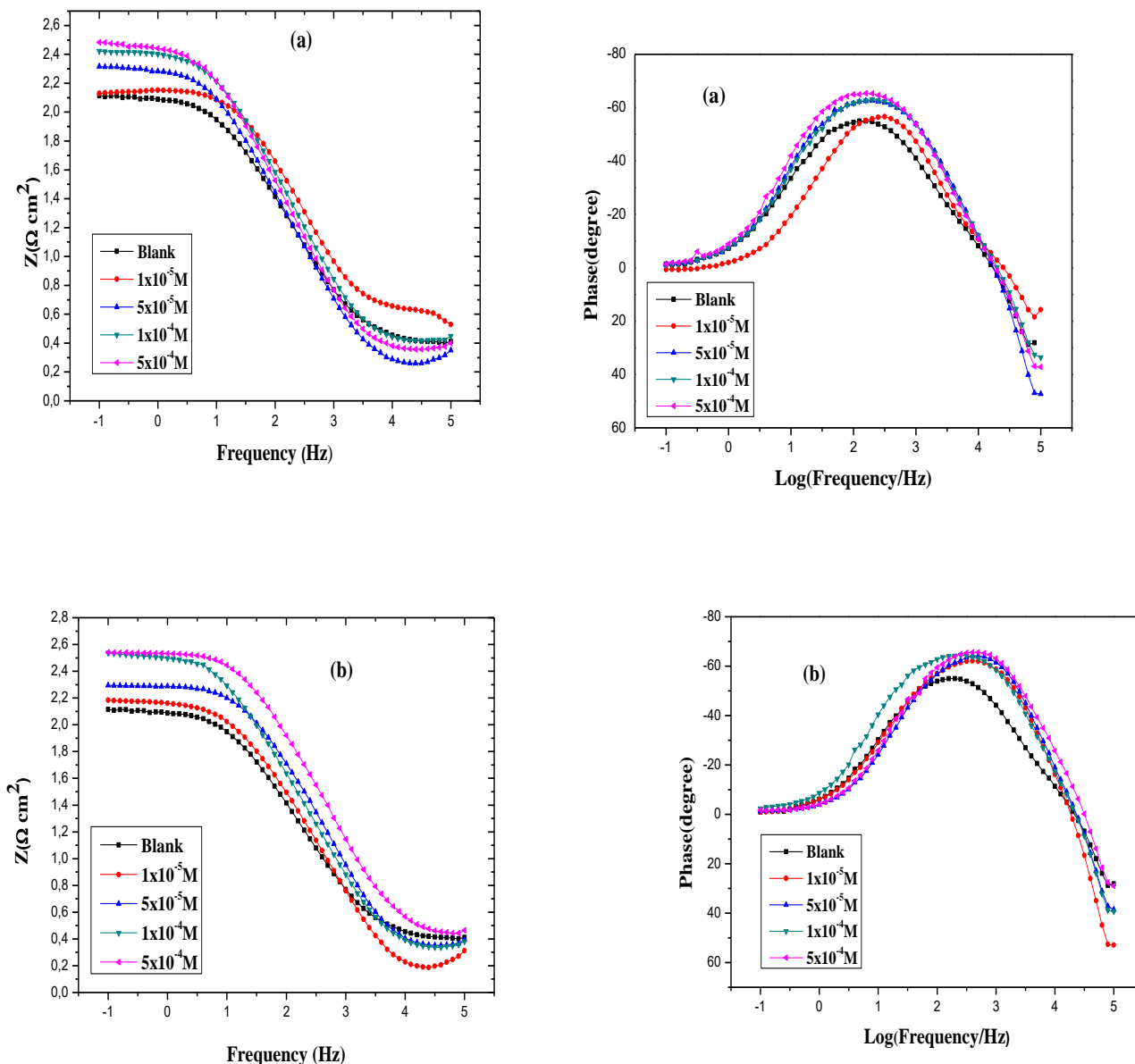
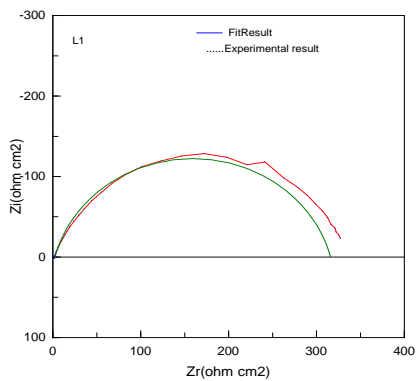
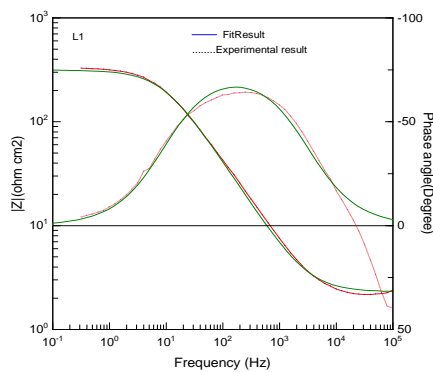


**Figure 8.** Bode and phase angle plots in absence and presence of various concentrations of (a) L1 and (b) L2.

(a)



(b)



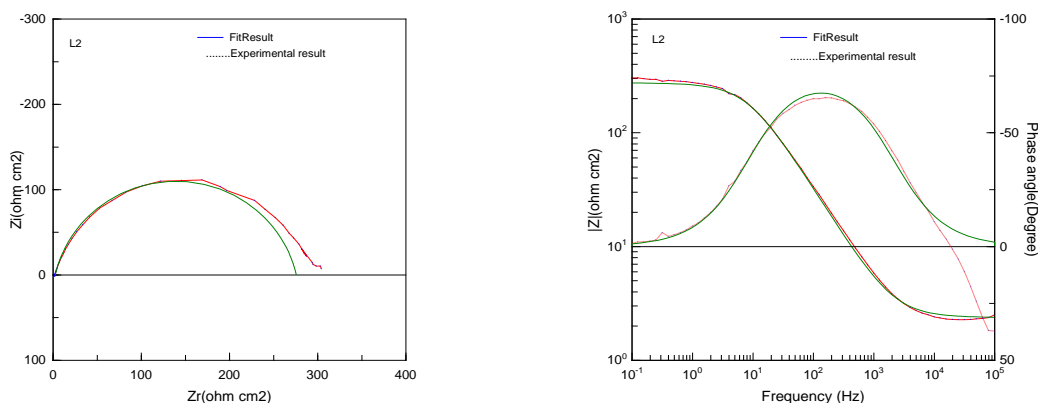


**Figure 9.** Impedance diagrams with  $5 \times 10^{-4}$  M of the studied Schiff bases L1 and L2 (a) Nyquist plot and (b) Bode plot; (.....) experimental result; (—) fit result.

As an example, the Nyquist and Bode plots of both experimental and simulated data of mild steel in uninhibited and inhibited acid solutions containing optimum concentrations of L1 and L2 are shown in Fig. 9 (a) and (b).

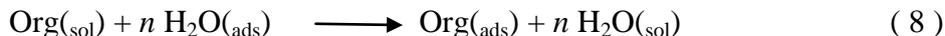
**Table 3.** The Electrochemical Impedance parameters and inhibition efficiency of mild steel in 1 M HCl containing different concentrations of L1 and L2.

<i>Inhibitor</i>	<i>C</i> ( <i>M</i> )	<i>R<sub>ct</sub></i> ( $\Omega \text{ Cm}^2$ )	<i>C<sub>dl</sub></i> ( $\mu\text{F/cm}^2$ )	<i>IE<sub>imp</sub></i> (%)	$\theta$
1M HCl(Blank)	-	21.63	132	-	-
4,4'-bis(2,4-dihydroxybenzaldehyde) diphenylethanediiimine (L1)	$1 \times 10^{-5}$	149.17	66.81	85.49	0.85
	$5 \times 10^{-5}$	201.20	60.21	89.24	0.89
	$1 \times 10^{-4}$	322.23	40.60	93.28	0.93
	$5 \times 10^{-4}$	343.54	24.95	93.70	0.93
4,4'-bis(4-diethylaminosalicylaldehyde) diphenylethanediiimine (L2)	$1 \times 10^{-5}$	136.09	79.34	83.51	0.83
	$5 \times 10^{-5}$	198.52	69.49	89.24	0.89
	$1 \times 10^{-4}$	259.65	60.68	91.67	0.91
	$5 \times 10^{-4}$	286.24	45.39	92.64	0.92

### 3.6. Adsorption isotherm

The adsorption of inhibitors on the metal surface is generally influenced by the chemical structure of the organic compounds, the charge distribution in the molecules, the nature of the surface-charged metals, the temperature and the types of media used. In fact, the solvent H<sub>2</sub>O molecules could

also adsorb at metal/solution interface [61]. The adsorption of organic inhibitor molecules from the aqueous solution can be regarded as a quasi-substitution process between the organic compounds in the aqueous phase [ $\text{Org}_{(\text{sol})}$ ] and water molecules at the electrode surface [ $\text{H}_2\text{O}_{(\text{ads})}$ ] as represented in Eq. (8)



Where  $n$  is the size ratio representing the number of water molecules replaced by one organic adsorbate. For organic inhibitors which possess the ability to adsorb on metal surface, the impeding dissolution reaction and the surface coverage can be evaluated as the inhibition efficiency. The relationship between the inhibition efficiency and the concentration of the inhibitor at constant temperature, which is known as isotherm, gives an insight into the adsorption process [62]. Several adsorption isotherms were attempted to fit  $\theta$  values to various isotherms including Frumkin [63], Temkin [64], Freundlich [64], Floy-Huggins [66] and Langmuir isotherm [67]. All these models were used as primary criteria to select the best adsorption isotherm with the aid of correlation coefficient  $R^2$ . The degree of surface coverage ( $\theta$ ) for different concentrations was evaluated from the weight loss data. Langmuir adsorption isotherm is the best description of the adsorption behavior of the inhibitor on the mild steel surface [68]. This isotherm can be represented by the following equation:

$$\frac{C_{inh}}{\theta} = \frac{1}{K_{ads}} + C_{inh} \quad (9)$$

In the cases of these plots the  $C_{inh}$  represents the concentration of the inhibitor,  $\theta$  is the fractional surface coverage and  $K_{ads}$  is the equilibrium constant for adsorption–desorption process. The relation between  $C_{inh} / \theta$  and  $C_{inh}$  in 1 M HCl at 25°C is shown in Fig. 10, and the expected linear relationship is observed with a strong correlation coefficients ( $R^2 = 0.99998$ ) for L1 and L2, respectively. From the intercept of the Langmuir plot, values of  $K_{ads}$  were calculated at different studied temperatures; ( $599.370 \times 10^{-5}$  M for L1 and  $641.02 \times 10^{-5}$  for L2 at 298 K). It should be noted that other adsorption isotherms including Langmuir, Temkin and Frumkin were made to fit the  $\theta$  values. In the present study, the Langmuir adsorption isotherm was tested and shows the best approximate between them. This is why the assumption is true for Langmuir adsorption isotherm. The value of the regression coefficient  $R^2$  established the validity of this approach. The slope of the straight line (1.02337 and 1.04367 for L1 and L2, respectively) is may be due to the adsorbed inhibitor molecules form monolayer on the steel surface and there is no interaction among the adsorbed Schiff base molecules.

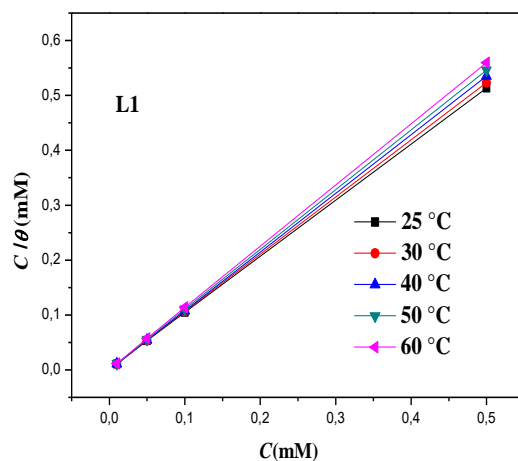
There is a good correlation between adsorption equilibrium constant ( $K_{ads}$ ) and standard free energy of adsorption ( $\Delta G_{ads}^0$ ) which is as follows:

$$K_{ads} = \frac{1}{55.5} \exp\left(-\frac{\Delta G_{ads}^0}{RT}\right) \quad (10)$$

The constant value of 55.5 denotes the concentration of water in solution,  $R$  is the universal gas constant and  $T$  is the temperature. The derived value of free energies ( $\Delta G^\circ_{ads}$ ) and  $K_{ads}$  for the studied Schiff bases are listed in Table 4. The relatively high value of adsorption equilibrium constant reflects the high adsorption ability on the mild steel surface.  $\Delta G^\circ_{ads}$  can be calculated from  $K_{ads}$ . The calculated values of  $\Delta G^\circ_{ads}$  were found as -25.79 and -25.96 kJ/mol designated for L1 and L2, respectively at  $5 \times 10^{-4}$  M for 25-60°C temperature range. The decreasing values of  $\Delta G^\circ_{ads}$  reflect the stronger ability of adsorption of the inhibitor. In this case, the negative values of  $\Delta G^\circ_{ads}$  indicate that both inhibitors are adsorbed spontaneously from HCl solution onto the mild steel surface. In general, when  $\Delta G^\circ_{ads}$  Values is in the order of -20 kJ/mol or more positive are associated with an electrostatic interaction between charged inhibitor molecule and charged metal surface, physisorption; and -40 kJ/mol or more negative values of  $\Delta G^\circ_{ads}$  is related to electron sharing or transfer from organic molecules to the metal surface to form a coordinate covalent bond, chemisorption. The values of  $\Delta G^\circ_{ads}$  for both compounds indicate physisorption on steel surface in acid solution [69]. The value of  $\Delta H^\circ$  and  $\Delta S^\circ$  can be calculated using van't-Hoff equation:

$$\ln K_{ads} = \ln \frac{1}{55.5} - \frac{\Delta H^\circ_{ads}}{RT} + \frac{\Delta S^\circ_{ads}}{R} \quad (11)$$

Where  $\Delta H^\circ$  the apparent enthalpy of adsorption and  $\Delta S^\circ$  the apparent entropy of adsorption, respectively. The relationship between  $\ln(K_{ads})$  and  $1/T$  gave a straight line with a slope of  $(-\Delta H^\circ_{ads}/R)$  and intercept equal to  $[\Delta S^\circ_{ads}/R + \ln(1/55.5)]$ , from which the value of  $\Delta H^\circ_{ads}$  and  $\Delta S^\circ_{ads}$  were calculated and presented in Table 4. Thermodynamic parameters for the adsorption of inhibitors can provide valuable information about the mechanism of corrosion inhibition. While an endothermic adsorption process ( $\Delta H^\circ_{ads} > 0$ ) is attributed unequivocally to chemisorption, an exothermic adsorption process ( $\Delta H^\circ_{ads} < 0$ ) may involve either physisorption or chemisorption or a mixture of both the processes [70, 71]. In an exothermic process, physisorption can distinguished from chemisorption by considering the absolute value of  $\Delta H^\circ_{ads}$ .



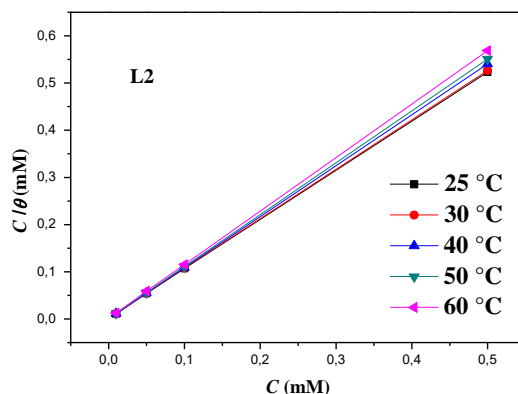


**Figure 10.** Langmuir isotherm plots for L1 and L2 on mild steel surface in 1 M HCl solution at different temperatures.

Furthermore, if the value of  $\Delta H^{\circ}_{ads} < 41.86$  kJ/mol then it is physisorption. While for chemisorption process,  $\Delta H^{\circ}_{ads}$  values in and around 100 kJ/mol. In the case of L1 and L2, the enthalpy value positive reflect that inhibitors adsorb onto the mild steel through endothermic reaction. That is the reason of the decrease in %IE with temperature. The positive sign of  $\Delta S^{\circ}_{ads}$  is also related to substitutional process, which can be attributed to the increase in the solvent entropy and more positive water desorption entropy. It also interpreted with increase of disorders due to the more water molecules which can be desorbed from the metal surface by one inhibitor molecule [72- 74].

**Table 4.** The values of  $K_{ads}$ ,  $\Delta G^{\circ}_{ads}$ ,  $\Delta H^{\circ}_{ads}$  and  $\Delta S^{\circ}_{ads}$  for steel obtained from Langmuir adsorption isotherm for the studied Schiff bases in 1M HCl at different temperatures.

Inhibitor	Temperature (K)	R <sup>2</sup>	K <sub>ads</sub> (mM <sup>-1</sup> )	ΔG <sup>o</sup> <sub>ads</sub> (Kj mol <sup>-1</sup> )	ΔH <sup>o</sup> <sub>ads</sub> (Kj mol <sup>-1</sup> )	ΔS <sup>o</sup> <sub>ads</sub> (j mol <sup>-1</sup> K <sup>-1</sup> )
L1	298	0.99998	599.37	-25.79	21.43	158.26
	303	0.99999	730.83	-26.78		
	313	1.00000	746.26	-29.37		
	323	0.99999	1154.10	-29.54		
	333	0.99998	1537.98	-29.72		
L2	298	0.99998	641.02	-25.96	22.14	160.19
	303	0.99998	628.93	-26.48		
	313	0.99999	662.25	-28.66		
	323	1.00000	1096.60	-28.96		
	333	1.00000	1590.63	-30.58		

### 3.7. Effect of temperature

Many changes occur on the metal / solution interface, such as desorption of inhibitors and the decomposition or rearrangement of inhibitor itself. This is the result of the impact of temperature on the corrosion process of metal in aggressive solution. The effect of temperature on the inhibition efficiency of Schiff base molecules was studied by weight loss measurements in the temperature range 303–333 k in absence and presence of inhibitors at optimum concentrations [75-78]. The results are

presented in Table 5. The data obtained suggest that all Schiff bases get adsorbed on the mild steel surface for all the temperatures studied and as the temperature increases, the corrosion rate increases in absence and presence of inhibitors and hence the values of the inhibition efficiency are found to decrease from 95.58% to 89.34% for L1 and from 94.93% to 87.90% for L2. These results confirm that all Schiff base molecules are excellent inhibitors in the range of temperature studied [79]. This decrease in inhibition is due to desorption of adsorbed inhibitors from metal surface and decomposition at elevated temperature [80]. Though there is no much difference between the IE (%) of the inhibitors, and the order for inhibition efficiency at the temperature is as follows: L1 > L2.

**Table 5.** Weight loss parameters such as Corrosion rate ( $W$ ) and corrosion inhibition ( $IE\%$ ) for mild steel in 1 M HCl at inhibitors optimum concentration ( $5 \times 10^{-4}$  M) in different temperatures derived from weight loss measurements.

<i>Inhibitor</i>		<i>Temperature (K)</i>			
		<b>303</b>	<b>313</b>	<b>323</b>	<b>333</b>
Blank	$W_0(mg\ cm^{-2}\ h^{-1})$	0.634	1.494	2.299	3.738
Schiff base L1	$W(mg\ cm^{-2}\ h^{-1})$	0.028	0.098	0.193	0.34
	<b>IE(%)</b>	<b>95.58</b>	<b>93.44</b>	<b>91.60</b>	<b>89.34</b>
Schiff base L2	$W(mg\ cm^{-2}\ h^{-1})$	0.0321	0.112	0.212	0.452
	<b>IE(%)</b>	<b>94.93</b>	<b>92.41</b>	<b>90.77</b>	<b>87.90</b>

### 3.8. SEM Analysis

The surface morphology was carried out for the MS surface immersed in 1 M HCl solution in the absence and presence of optimum concentration  $5 \times 10^{-4}$  M of the Schiff bases L1 and L2. This establishes the interaction of the inhibitor molecules with the surface. The experimental results were gathered in Fig. 11, from which, the surface MS sample seemed smooth before immersion (Fig. 11a) but Fig. 11(b) shows the SEM image of the mild steel surface after immersion in the acid without inhibitory molecule for 6 h [81, 82]. It was obvious that the specimen in the absence of inhibitors was seriously corroded and the unprotected metal surface contains a number of pits and cavities (rapid corrosion attack). From (Figure 11(c)-11(d)) it can be concluded that the surface of the corroded area of the mild steel immersed in hydrochloric acid solution is remarkably improved with the addition of the Schiff bases and the presence of the inhibitors exhibited a smooth surface indicating restricted corrosion unlike Fig. 11b. The SEM images clearly indicate that the mild steel surface was protected from the corrosion in the presence of Schiff bases L1 and L2, which are acting as corrosion inhibitors. These results are in conformity with the observed inhibition efficiency values of other methods such as electrochemical measurements.

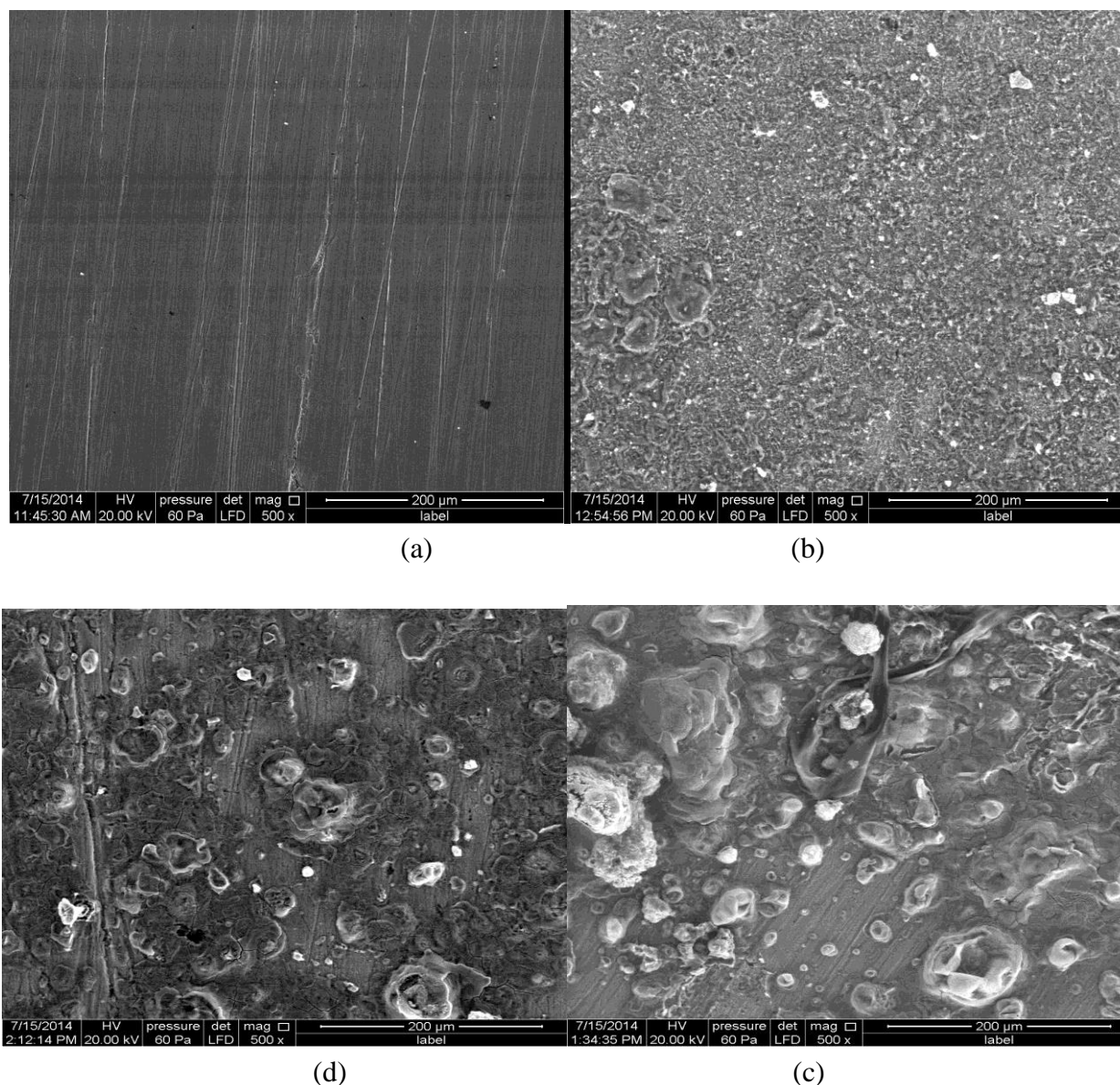


**Figure 11.** SEM images of (a) MS surface, (b) MS in 1.0 M HCl, (c) MS in 200 μm Schiff base (L1), (d) MS in 200 μm Schiff base (L2).

#### 4. QUANTUM CHEMICAL CALCULATIONS

Use of quantum chemical calculations is very important in studying the correlation between molecular structure and corrosion inhibition efficiency [83]. Moreover, a theoretical study permits the pre-selection of compounds with the necessary structural characteristics to act as organic corrosion inhibitors. Thus, several corrosion publications have incorporated these theoretical approaches [84, 85]. In order to support the experimental findings obtained for the studied Schiff base molecules, quantum chemical parameters, namely the energy of highest occupied molecular orbital ( $E_{HOMO}$ ), energy of the lowest unoccupied molecular orbital ( $E_{LUMO}$ ), the energy gap ( $E_{LUMO} - E_{HOMO}$ ), dipole ( $\mu$ ), Ionization Potential (I), Electron Affinity (A), electronegativity ( $\chi$ ), global hardness ( $\eta$ ) and the

fraction of electron transferred ( $\Delta N$ ) from the inhibitor molecules to iron are listed in Table 6. All of theoretical calculations were obtained after geometric optimization using Kohn-Sham approach at DFT level. Optimized molecular structure, the HOMO density distribution, the LUMO density distribution of the Schiff bases L1 and L2 obtained with DFT at the B3LYP/6-31G (d, p) level of theory are shown in Fig. 12. It can be seen that the electron density of the HOMO and LUMO location in the molecules is mainly distributed near the nitrogen (NH) and hydroxyl (OH) atoms and on the rings benzene. This indicates that are the favorite sites for adsorption. The molecular structure of the Schiff bases has shown that they can adsorb on the surface of the steel by dividing the electron of the nitrogen atoms with the metal surface to form coordinated bonds and  $\pi$ -electron interactions of the aromatic rings. It is known that in the chemical adsorption, an increase in  $E_{HOMO}$  causes significant increase in inhibition efficiency of organic compounds while the negative sign of HOMO coefficient has been interpreted by some researchers to be an indication of physical rather than chemical adsorption [86-88]. Therefore, increasing values of  $E_{HOMO}$  of the molecule means a higher tendency for the donation of electron(s) to the appropriate acceptor molecules with low-energy empty molecular orbital. The inhibition efficiency also increases with decreasing LUMO energy of the inhibitors. It is known that,  $E_{LUMO}$  indicates the ability of the molecule to receive electrons. Excellent corrosion inhibitors are usually those organic compounds, which did not only offer electrons to unoccupied orbital of the metal, but also accept free electrons from the metal [89]. In the present study, The HOMO energy value is (-5.30 eV) for L2 and (-4.84 eV) for L1, illustrating that L1 has strong electron donating than L2. The obtained value of the LUMO energy is equal to (-1.25 eV) indicates the easier of the acceptance of more electrons from the d orbital of the metal leading to the formation of a feedback bond [90]. The band gap energy,  $E_{LUMO} - E_{HOMO}$  is an important parameter as a function of the reactivity of the inhibitor molecule which determines the interaction between the adsorbed inhibitor and the metallic substrate. The calculations indicate that L1 exhibits the smaller energy gap (4.00 eV), which means as energy gap decreases, the chemical reactivity of the molecule increases and will providing good inhibition efficiencies. The dipole moment ( $\mu$  in Debye) is an important electronic parameter which results from the non- uniform distribution of the charges on the different atoms of the molecule. Inhibitor with high dipole moment tends to form strong dipole-dipole interactions with the metal leading to greater inhibition efficiency. In our study, the calculated dipole moment values for L1 (1.55 Debye) and L2 (1.29 Debye) show that L2 can be probably adsorbed on the steel surface more easily than L1 which agrees well with the experimental findings [91]. Other quantum chemical parameters including the fraction of electronic charge transferred ( $\Delta N$ ) from the inhibitor to the metal is another important factor depending on the quantum chemical method, may be written as:

$$\Delta N = \frac{\chi_M - \chi_I}{2(\eta_M + \eta_I)} \quad (12)$$

Where the subscripts  $\chi_M$  and  $\chi_I$  represent the absolute electronegativity of metal and inhibitor molecule, respectively;  $\eta_M$  and  $\eta_I$  represent the absolute hardness of metal and the inhibitor molecule, respectively. These quantities are related to the reactivity and selectivity of the inhibitors like ionization potential (I), electron affinity (A) and were estimated according to Koopman's theorem [92].

$$\chi = \frac{I + A}{2} \quad (13)$$

$$\eta = \frac{(I - A)}{2} \quad (14)$$

Ionization potential (I) is related to the energy of the  $E_{HOMO}$  through the equation:

$$I = -E_{HOMO} \quad (15)$$

Electron affinity (A) is related to  $E_{LUMO}$  through the equation:

$$A = -E_{LUMO} \quad (16)$$

According to Pearson [93], operational and approximate of the electronic chemical potential ( $\mu$ ) of a chemical system is defined follows.

$$-\mu = \frac{(I + A)}{2} = \chi \quad (17)$$

Where  $(I+A)/2$  is the Mulliken electronegativity for atoms, the electrophilicity is a descriptor of reactivity that allows a quantitative classification of the global electrophilic nature of a molecule within a relative scale. Parr et al. [94], have proposed electrophilicity index as a measure of energy lowering due to maximal electron flow between donor and acceptor through the equation:

$$\omega = \frac{\chi^2}{2\eta} \quad (18)$$

This was proposed as a measure of the electrophilic power of a molecule. Global softness ( $\sigma$ ), describes the capacity of an atom or group of atoms to receive electron [95], it can also be defined by using the equation:

$$\sigma = \frac{1}{\eta} \quad (19)$$

The percent inhibition of steel with Schiff base inhibitors shows good correlation with the electronic chemical potential, as depicted in Fig. 12. Using a theoretical  $\chi_M$  value of 7 eV mol<sup>-1</sup> and  $\eta_M$  value of 0 eV mol<sup>-1</sup> for iron atom [96]. In this study,  $\Delta N$ , the fraction of electrons transferred from

inhibitor to the iron molecule, was calculated and given in Table 6. The values of the obtained  $\Delta N$  clearly reveal that the inhibition efficiency increases with the  $\Delta N$  increase, agreeing with literature [97], if  $\Delta N < 3.6$ , the inhibition efficiency increases by increasing electron-donating ability of these inhibitors to donate electrons to the metal surface, while it decreased if  $\Delta N > 3.6$  (electron). The results indicate that Schiff bases L1 and L2 are the donors of electrons, and the metal surface is the acceptor of electrons. The compounds are bound to the metal surface, and thus form an inhibition adsorption layer against corrosion at mild steel/hydrochloric acid solution interface. The calculated values of global hardness, softness and electrophilicity index are given in Table 6. It is reported that adsorption of inhibitor onto a metallic surface occurs at the part of the molecule which has the greatest softness and lowest hardness. Global softness ( $\sigma$ ) is also an important parameter describing the adsorption of inhibitor on the surface. In corrosion inhibition chemistry, the inhibitors are considered as soft base and the metals as soft acid [98]. Soft-soft interaction is the most predominant factor for the adsorption of inhibitor molecules.

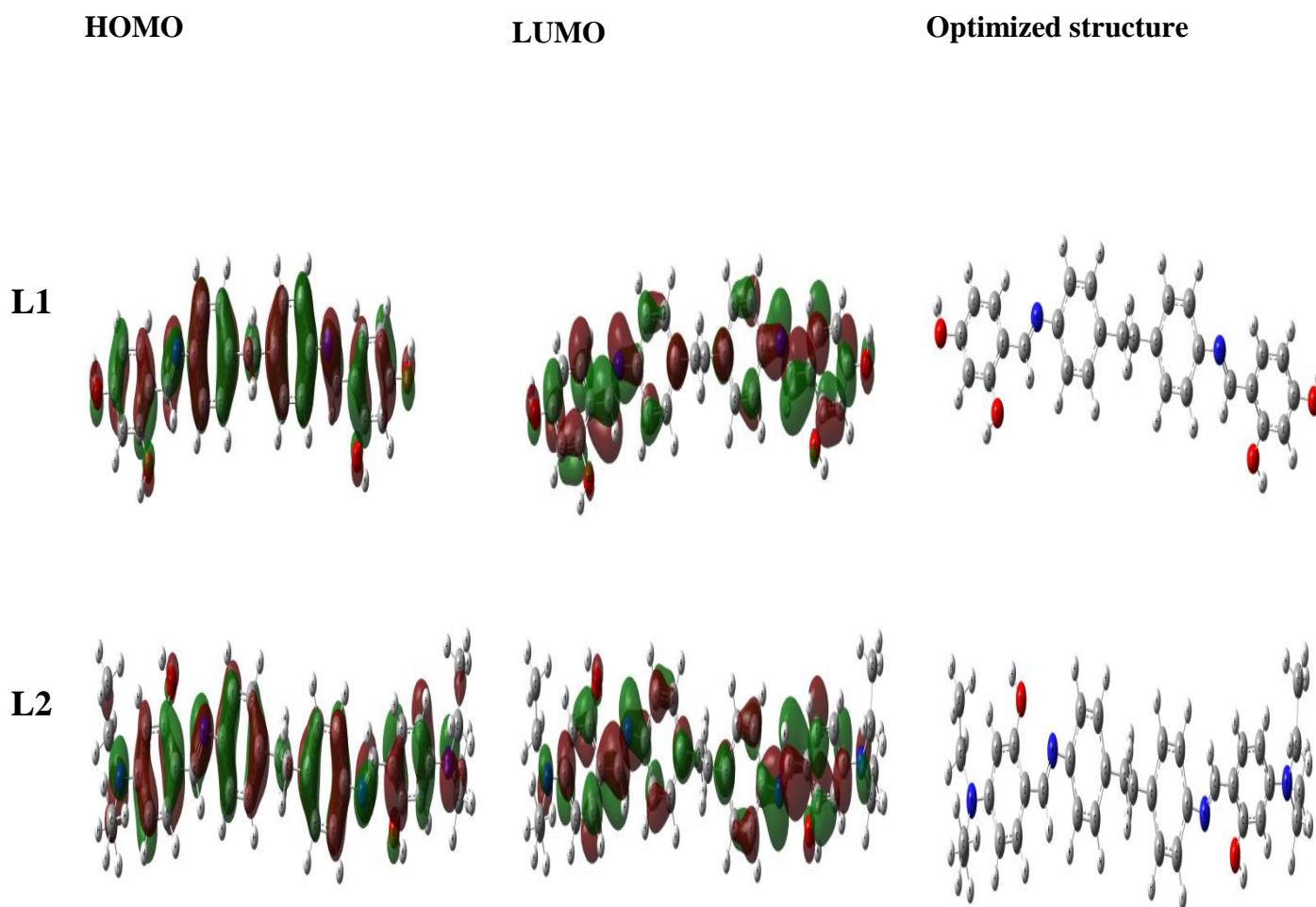


**Figure 12.** Repartition of HOMO, LUMO densities and optimized structures of the studied Schiff bases obtained from DFT at the B3LYP/6-31G (d, p) level.

Whereas, the high value of global softness consisted with high inhibition efficiency [99]. In our present study, the result presented in Table 6 shows that the inhibitor L1 has the lowest hardness value and the highest softness value is expected to be the best inhibitor and it is in well agreement with experimental inhibition efficiencies. According to this definition  $\omega$  measures the propensity of chemical species to accept electrons. Thus, a good nucleophile exhibit low values of  $\omega$ . On the other hand, a good electrophile is characterized by high values of  $\omega$ . The estimation of the adsorption centers of the inhibitors and the calculation of the distribution of the charges over the whole skeleton molecule have been widely reported by the use of the Mulliken population analysis [100-102]. Several authors have stated that there is a general consensus that the most negatively charged heteroatom, is the more it can be adsorbed on the metal surface through the donor-acceptor type reaction [103, 104]. Mulliken charges on heteroatoms of the inhibitors are located in Table 7. As it can be seen, highest negative charges are on the nitrogen and oxygen atoms; (-0.500 e, -0.561 e) for respectively N49 and O57 in L1, (-0.508 e, -0.522 e) for N50 and O81 in L2. The adsorption of the Schiff base molecules L1 and L2 on the mild steel would take place through the aromatic rings, the carbonyl and the functional groups like the imine and oxygen atom. This result suggests that L1 and L2 should behave as good corrosion inhibitors.

**Table 6.** Quantum chemical parameters for Schiff base molecules L1 and L2 calculated using DFT at the B3LYP/6-31G (d, p) basis set.

Molecule	$E_{\text{HOMO}}$ eV	$E_{\text{LUMO}}$ eV	$\Delta E_{\text{gap}}=(E_{\text{LUMO}}(\text{eV}) - E_{\text{HOMO}}(\text{eV}))$	Dipole moment $\mu$ Debye	Total energy $E_{\text{total}}(\text{a.u.})$	EA eV	IP eV	Electronegativity $\chi$ eV	Hardness $\eta$ eV	Softness ( $\sigma$ ) $\text{eV}^{-1}$	$\omega$	$\Delta N$	$IE_p\%$
L1	-4.84	-0.84	-4.00	1.55	-1491.85	0.84	4.84	2.84	2.00	0.50	2.016	1.04	95.33
L2	-5.30	-1.25	-4.04	1.29	-1766.62	1.25	5.30	3.27	2.02	0.495	2.646	0.92	94.18

#### 4.1. Active sites

Inhibitor molecules can bind with metal surface by electron transfer (donating or accepting). Therefore, in an inhibitor it is important to examine the active sites of interaction. To investigate the active sites of an inhibitor, there are three controlling factors that must be considered: (i) neutral atomic charge, (ii) distribution of frontier molecular orbitals and (iii) Fukui indices. In this study, local reactivity was investigated using the Fukui functions deduced through DFT [105, 106]. The active sites of molecule, which possess the largest condensed Fukui functions, favor the higher reactivity. These functions provide information about the reactive centers and indicate their chemical reactivity for nucleophilic and electrophilic nature [107-109]. The nucleophilic and electrophilic attacks are controlled by the maximum threshold values of  $f_k^+$  and  $f_k^-$ . The preferred sites for nucleophilic attacks are the atoms or the regions where the value of  $f_k^+$  is the highest; similarly, electrophilic attacks are preferred where the value of  $f_k^-$  is the largest.

**Table 7.** Mulliken atomic charges, the condensed Fukui functions on the selected atoms of the Schiff bases L1 and L2 calculated using DFT at the B3LYP/6-31+G (d) method.

<i>Inhibitor</i>	<i>Atoms</i>	$q_N$	$q_{N+1}$	$q_{N-1}$	$f_k^+$	$f_k^-$	$f_k^\bullet$
<b>L1</b>	C6	0.2462	0.2469	0.2524	0.0006	-0.0061	-0.0027
	C11	-0.2382	-0.2299	-0.2505	0.0082	0.0122	0.0102
	C29	0.1234	0.0766	0.1443	-0.0468	-0.0209	-0.0338
	C41	0.2910	0.2712	0.3081	-0.0198	-0.0171	-0.0184
	C43	-0.1573	-0.1683	-0.1467	-0.0109	-0.0105	-0.0107
	C46	0.3320	0.3037	0.3451	-0.0282	-0.0131	-0.0207
	N49	-0.5003	-0.5333	-0.4790	-0.0330	-0.0213	-0.0271
	N50	-0.5003	-0.5333	-0.4790	-0.0330	-0.0213	-0.0271
	O51	-0.5546	-0.5777	-0.5256	-0.0230	-0.0289	-0.0260
	O53	-0.5546	-0.5777	-0.5256	-0.0230	-0.0289	-0.0260
	O55	-0.5617	-0.5677	-0.5495	-0.0059	-0.0122	-0.0090
	O57	-0.5617	-0.5677	-0.5495	-0.0059	-0.0122	-0.0090
<b>L2</b>	C6	0.2401	0.2398	0.2405	-0.0002	-0.0003	-0.0003
	C24	0.2402	0.2394	0.2399	-0.0007	-0.0002	-0.0002
	C27	0.0957	0.0545	0.1062	-0.0141	-0.0105	-0.0258
	C29	0.0958	0.0542	0.1071	-0.0416	-0.0112	-0.0264
	C33	0.2792	0.2553	0.2930	-0.0238	-0.0138	-0.0188
	C36	-0.1857	-0.1916	-0.1726	-0.0059	-0.0130	-0.0094
	C37	0.3572	0.3290	0.3620	-0.0282	-0.0048	-0.0165
	C41	0.2790	0.2549	0.2934	-0.0241	-0.0143	-0.0192
	C46	0.3575	0.3295	0.3637	-0.0280	-0.0061	-0.0171
	C53	-0.0551	-0.0420	-0.0720	0.0131	0.0168	0.0150
	C60	-0.0538	-0.0412	-0.0701	0.0125	0.0163	0.0144
	C68	-0.3155	-0.3104	-0.3206	0.0050	0.0051	0.0050
	C74	-0.0535	-0.0407	-0.0698	0.0127	0.0162	0.0145
	N49	-0.5081	-0.5104	-0.4878	-0.0023	-0.0203	-0.0113
	N50	-0.5083	-0.5102	-0.4849	-0.0019	-0.0233	-0.0126
	N51	-0.4725	-0.5037	-0.4476	-0.0312	-0.0248	-0.0280
	N52	-0.4727	-0.5036	-0.4499	-0.0309	-0.0227	-0.0268
	O81	-0.5225	-0.5277	-0.5143	-0.0051	-0.0082	-0.0067
O83	-0.5224	-0.5275	-0.5143	-0.0050	-0.0080	-0.0065	

The Fukui function  $f_k$  has been formally defined as the first derivative of the electronic density  $\rho(r)$  with respect to the number of electrons  $N$  in a constant external potential  $v(r)$ .

$$f_k = \left( \frac{\delta \rho(\vec{r})}{\delta N} \right)_{v(\vec{r})} \quad (20)$$

Eq. (20) is indicated as the most standard presentation of the Fukui function. Owing to the discontinuity of the chemical potential at integer  $N$ , the derivative will be different if taken from the right or the left side. The Fukui function can be written by using the Mulliken population analysis (MPA) and the finite difference (FD) approximations approach as follows:

$$f_k^+ = q_k(N+1) - q_k(N) \quad (21)$$

$$f_k^- = q_k(N) - q_k(N-1) \quad (22)$$

$$f_k^o = \left[ \frac{q_k(N+1) - q_k(N-1)}{2} \right] \quad (23)$$

Where  $q_k(N)$ ,  $q_k(N+1)$ , and  $q_k(N-1)$  are the electronic population of the atom  $k$  in neutral, anionic and cationic systems respectively;  $f_k^+$  and  $f_k^-$  are the Fukui indices condensed on atom  $k$  and measure its electrophilic and nucleophilic tendencies respectively.

In this work, condensed Fukui functions were calculated using Mulliken atomic charges at DFT level of theories. The equations (21)-(23) were employed to calculate the value of the Fukui function atom by atom for the electrophilic, nucleophilic and free radical attack. Table 7 present calculated values of condensed Fukui functions (calculated from Mulliken charge distributions).

From the results obtained, we note the presence of negative values of the Fukui function. Recently it was reported that a negative Fukui function value describes the addition of an electron to the molecule, in some spots, the electron density is reduced; alternatively when removing an electron from the molecule, the electron density is increased [110]. For this study, the most probable reactive site for the adsorption of the studied inhibitors L1 and L2 is located on nitrogen and oxygen atoms and some carbon atoms which have the highest negative charge. When the molecule is accepting electrons, the system will have an  $f_k^+$ , the index for nucleophilic attack. On the other hand,  $f_k^-$  is the index for electrophilic attack when the molecule loss electrons. The results shown in Table 7 indicate that the preferred sites for electrophilic attacks as suggested by the values of  $f_k^-$  are O(51), and O(53) for L1 as well as N(49), N(50), N(51), N(52) attributed to L2. These sites present the highest values of  $f_k^-$ , e.g., -0.0289 for O(51), -0.0289 for O(53) and -0.0203 for N(49), -0.0233 for N(50), -0.0248 for N(51), -0.0227 for N(52). On the other hand, the values of  $f_k^+$  is highest on C(29), C(46), N(49), N(50) atoms for L1 and C(29), C(37), C(46), N(51), N(52) atoms for L2, indicating that these atoms are the most susceptible sites for nucleophilic attacks on the inhibitor; these sites have the highest values of  $f_k^+$ , e.g., -0.0468 for C(29), -0.0282 for C(46), -0.0330 for N(49), -0.0330 for N(50), and -0.0416 for C(29), -0.0282 for C(37), -0.0280 for C(46), -0.0312 for N(51), -0.0309 for N(52). The observed similarities in the sites suggest a same mechanism of inhibition. It should be noted that the nitrogen atom in both L1 and L2 molecules has large values of  $f_k^o$  on the site indicating that the nitrogen has a high availability for radical attack. From these results, there is confirmation on the possibility of donation and back-donation of electrons between inhibitors and steel surface. It was observed that

azomethine linkages are the most appropriate sites for nucleophilic attack, whereas oxygen and nitrogen atoms are appropriate for the electrophilic one. It can be concluded that the investigated compounds L1 and L2 have many active sites for the adsorption on the surface of mild steel. These results agree well with the experimentally inhibition efficiency.

## 5. CONCLUSIONS

1. Both Schiff bases, 4, 4'-bis(2,4-dihydroxybenzaldehyde)diphenylethanediiimine (L1) and 4,4'-bis(4-diethylaminosalicylaldehyde)diphenylethanediiimine (L2), were successfully synthesized and investigated as corrosion inhibitors using a series of techniques. These compounds exhibited excellent inhibition performance.

2. The results obtained from weight loss and electrochemical studies showed that the inhibiting properties increase with inhibitor concentrations but decreased with solution temperature. The IE% increases in accordance to the order: compound L1 > compound L2 for all the employed methods.

3. The results of Potentiodynamic polarization studies reveal that L1 and L2 influence both cathodic and anodic processes and hence behave as a mixed type inhibitors.

4. The Schiff bases L1 and L2 exhibited high inhibition efficiency than that of parent amine, 4,4'-diaminodiphenylethane (M1) for the studied concentrations.

5. Langmuir adsorption isotherm was found to be the best description for the studied inhibitors, and involves physical adsorption mechanism.

6.  $K_{ads}$  values show that both molecules tend adsorption towards on the mild steel surface. The values of  $\Delta G_{ads}$  could be attributed to the adsorption capability of the inhibitor molecules with the metal surface, forming a protective film.

7. Scanning electron microscopy (SEM) and energy dispersive X-ray spectroscopy (EDX) were performed to characterize the passive film on the metal surface.

8. The condensed Fukui functions describe in detail the electrophilic as well as the nucleophilic attacking the centers, where the corresponding electrophilic and nucleophilic interaction may occur providing the information about the reactivity of the molecules. The theoretical calculations are consistent with those of the experimental work.

## References

1. F. Bentiss, C. Jama, B. Mernari, H. El Attari, L. El Kadi, M. Lebrini, M. Traisnel, M. Lagrenée, *Corros. Sci.* 51(2009) 1628.
2. H. Wang, H. Fan, J. Zheng, *Mater. Chem. Phys.* 77 (2003) 655.
3. S. A. A. El-Maksoud, A. S. Fouda, *Mater. Chem. Phys.* 93 (2005) 84.
4. C. C. Nathan, *Corrosion Inhibitors (National Association of Corrosion Engineers), Houston, Texas*, (1981)
5. I. Zaafarany, *Port. Electrochim. Acta.* 27 (2009) 631.
6. J. Aljourani, K. Raeissi, M.A. Golozar, *Corros. Sci.* 51 (2009) 1836.
7. M. L. Zheludkevich, K. A. Yasakau, S. K. Poznyak, M. G. S. Ferreira, *Corros. Sci.* 47 (2005) 3368.

8. I. B. Obot, N. O. Obi-Egbedi, S. A. Umoren, *Corros. Sci.* (2) 51 (2009) 276.
9. M.G. Hosseini, M. Ehteshamzadeh, T. Shahrabi, *Electrochim. Acta.* 52 (2007) 3680.
10. M.N. Desai, M.B. Desai, C.B. Shah, S.M. Desai, *Corros. Sci.* 26 (1986) 827.
11. H. D. Lece, K.C. Emregul, O. Atakol, *Corros. Sci.* 50 (2008) 1460.
12. H. Keles, M. Keles, I. Dehri, O. Serindag, *Colloids Surf. A Physicochem. Eng. Aspects.* 320 (2008) 138.
13. M. Behpour, S.M. Ghoreishi, N. Soltani, M. Salavati-Niasari, *Corros. Sci.* 51 (2009) 1073.
14. E. Naderi, A.H. Jafari, M. Ehteshamzadeh, M.G. Hosseini, *Mater. Chem. Phys.* 115 (2009) 852.
15. A. Aytac, U. Ozmen, M. Kabasakaloglu, *Mater. Chem. Phys.* 89 (2005) 176.
16. S. L. Li, H.Y. Ma, S.B. Lei, R. Yu, S.H. Chen, D.X. Liu, *Corrosion.* 54 (1998) 947.
17. S. Li, S. Chen, S. Lei, H. Ma, R. Yu, D. Liu, *Corros. Sci.* 41 (1999) 1273.
18. K. C. Emregül, M. Hayvali, *Corros. Sci.* 48 (2006) 797.
19. F. Bentiss, M. Bouanis, B. Mernari, M. Traisnel, H. Vezin, M. Lagrenee, *Appl. Surf. Sci.* 253 (2007) 3696.
20. K.C. Emregül, E. Düzgün, O. Atakol, *Corros. Sci.* 48 (2006) 3243.
21. H. Ju, Z. P. Kai, Y. Li, *Corros. Sci.* 50 (2008) 865.
22. M. A. Hegazy, *Corros. Sci.* (11) 51 (2009) 2610.
23. I. Danaee, O. Ghasemi, G. R. Rashed, M. Rashvand Avei, M.H. Maddahy, *J. Mol. Struct.* 1035 (2013) 247.
24. C. M. Goulart, A. E. Souza, C. A. M. Huitle, C. J. F. Rodrigues, M. A. M. Maciel, A. Echevarria, *Corros. Sci.* 67 (2013) 281.
25. S. Issaadi, T. Douadi, S. Chafaa, *Appl. Surf. Sci.* 316 (2014) 582.
26. H. Hamani, T. Douadi, M. Al-Noaimi, S. Issaadi, D. Daoud, S. Chafaa, *Corros. Sci.* 88 (2014) 234.
27. D. Daoud, T. Douadi, H. Hamani, S. Chafaa, M. Al-Noaimi, *Corros. Sci.* 94 (2015) 21.
28. Y. Sharma, H.N. Pandey, P. Mathur, *Polyhedron.* 13 (1994) 3111.
29. I.B. Obot, N.O. Obi-Egbedi, *Colloids Surf. A: Physicochem. Eng. Asp.* 330 (2008) 207.
30. K. C. Emregül, O. Atakol, *Mater. Chem. Phys.* 83 (2004) 373.
31. X.H. Li, S.D. Deng, H. Fu, G.N. Mu, N. Zhao, *Appl. Surf. Sci.* 254 (2008) 5574.
32. H. Amar, T. Braisaz, D. Villemin, B. Moreau, *Mater. Chem. Phys.* 110 (2008) 1.
33. H. Zarrok, A. Zarrouk, B. Hammouti, R. Salghi, C. Jama, F. Bentiss, *Corros. Sci.* 64 (2012) 243.
34. Gaussian 03, Revision B.01, M. J. Frisch, G.W. Trucks, H.B. Schlegel, G.E. Scuseria, M.A. Robb, J.R. Cheeseman, J.A. Montgomery, Jr., T. Vreven, K.N. Kudin, J.C. Burant, J.M. Millam, S.S. Iyengar, J. Tomasi, V. Barone, B. Mennucci, M. Cossi, G. Scalmani, N. Rega, G.A. Petersson, H. Nakatsuji, M. Hada, M. Ehara, K. Toyota, R. Fukuda, J. Hasegawa, M. Ishida, T. Nakajima, Y. Honda, O. Kitao, H. Nakai, M. Klene, X. Li, J.E. Knox, H.P. Hratchian, J.B. Cross, C. Adamo, J. Jaramillo, R. Gomperts, R.E. Stratmann, O. Yazyev, A.J. Austin, R. Cammi, C. Pomelli, J.W. Ochterski, P.Y. Ayala, K. Morokuma, G.A. Voth, P. Salvador, J.J. Dannenberg, V.G. Zakrzewski, S. Dapprich, A.D. Daniels, M.C. Strain, O. Farkas, D.K. Malick, A.D. Rabuck, K. Raghavachari, J.B. Foresman, J.V. Ortiz, Q. Cui, A.G. Baboul, S. Clifford, J. Cioslowski, B.B. Stefanov, G. Liu, A. Liashenko, P. Piskorz, I. Komaromi, R.L. Martin, D.J. Fox, T. Keith, M.A. Al-Laham, C.Y. Peng, A. Nanayakkara, M. Challacombe, P.M.W. Gill, B. Johnson, W. Chen, M.W. Wong, C. Gonzalez, J.A. Pople, *Gaussian, Inc., Pittsburgh PA*, (2003).
35. A. D. Becke, *J. Chem. Phys.* 84 (1986) 4524.
36. A. D. Becke, *J. Chem. Phys.* 98 (1993) 5648.
37. C. Lee, W. Yang, R.G. Parr, *Phys. Rev. B* 37 (1998) 785.
38. H. Ashassi-Sorkhabi, B. Shaabani, D. Seifzadeh, *Electrochim. Acta.* 50 (2005) 3446.
39. K. Stanly Jacob, Geetha Parameswaran, *Corros. Sci.* 52 (2010) 224.
40. N. Kuriakose, J. T. Kakkassery, V. P. Raphael, S. K. Shanmughan, *Indian J. Mater. Sci.* 2014 (2014) 6.

41. I. Ahamad, R. Prasad, M.A. Quraishi, *Corros. Sci.* 52 (2010) 933.
42. I.N. Putilova, S.A. Balezin, U.P. Baranik, *Pergamon Press, New York.* (1960) 31.
43. K.F. Khaled, *Corros. Sci.* 52 (2010) 2905.
44. D.K. Yadav, M.A. Quraishi, B. Maiti, *Corros. Sci.* 55 (2012) 254.
45. S. Issaadi, T. Douadi, A. Zouaoui, S. Chafaa, M.A. Khan, G. Bouet, *Corros. Sci.* 53 (2011) 1484.
46. W.A.W. Elyn Amira, A.A. Rahim, H. Osman, K. Awang, P. Bothi Raja, *Int. J. Electrochem. Sci.* 6 (2011) 2998.
47. M.A. Amin, M.A. Ahmed, H.A. Arida, T. Arslan, M. Saracoglu, F. Kandermirli, *Corros. Sci.* 53 (2011) 540.
48. M. Belayachi, H. Serrar, H. Zarrok, A. El Assyry, A. Zarrouk, H. Oudda, S. Boukhris, B. Hammouti, E. E. Ebenso, A. Geunbour, *Int. J. Electrochem. Sci.* 10 (2015) 3010.
49. O. L. Riggs, *Corrosion inhibitors*, C. C. Nathan, NACE, Houston, TX, 2nd ed. (1973) 7.
50. M. Mohammad, R.T. Ali, H. Krister, *J. Surf. Deterg.* 14 (2011) 605.
51. E. P. Manuel, O. Crescencio, V. L. Natalya, J. Boanerge, *J. Surf. Deterg.* 14 (2011) 211.
52. A. Yurt, A. Balaban, S. Kandemir, G. Bereket, B. Erk, *Materials Chemistry and Physics.* 85(2004) 420.
53. A. K. Singh, S. K. Shukla, M. Singh, M. A. Quraishi, *Materials Chemistry and Physics.* 129 (2011) 68.
54. E. McCafferty, N. Hackerman, *J. Electrochem. Soc.* 119 (1972) 146.
55. S. L. Ashok Kumar, M. Gopiraman, M. S. Kumar, A. Sreekanth, *Ind. Eng. Chem. Res.* 50 (2011) 7824.
56. M. Lagrenee, B. Mernari, M. Bouanis, M. Traisnel, F. Bentiss, *Corros. Sci.* 44 (2002) 573.
57. E. E. Ebenso, U. J. Ekpe, B. I. Ita, O. E. Offiong, U. J. Ibok, *Mater. Chem. Phys.* 60 (1999) 79.
58. M.A. Veloz, I. Gonzalez, *Electrochim. Acta.* 48 (2002) 135.
59. M. Mahdavian, S. Ashhari, *Electrochim. Acta.* 55 (2010) 1720.
60. Y. J. Tan, S. Bailey, B. Kinsella, *Corros. Sci.* 38 (1996) 1545.
61. L. Narvaez, E. Cano, D.M. Bastidas, *J. Appl. Electrochem.* 35 (2005) 499.
62. W.H. Durnie, B.J. Kinsella, R. deMarco, A. Jefferson, *J. Appl. Electrochem.* 31 (2001) 1221.
63. E.E. Oguzie, Y. Li, F.H. Wang, *J. Colloid Interface Sci.* 310 (2007) 90.
64. P.C. Okafor, Y. Zheng, *Corros. Sci.* 51 (2009) 850.
65. I.B. Obot, N.O. Obi-Egbedi, *Corros. Sci.* 52 (2010) 198.
66. P. J. Flory, *J. Chem. phys.* 10 (1942) 51.
67. P.C. Okafor, C.B. Liu, X. Liu, Y.G. Zheng, F. Wang, C.Y. Liu, F. Wang, *J. Solid State Electrochim.* 14 (2010) 1367.
68. P. Roy, A. Pal, D. Sukul, *RSC Adv.* 4 (2014) 10607.
69. D. K. Yadav, M. A. Quraishi, *Ind. Eng. Chem. Res.* 51 (2012) 8194.
70. F. Bentiss, M. Lebrini, M. Lagrenée, *Corros. Sci.* 47 (2005) 2915.
71. A. Kosari, M. Momeni, R. Parvizi, M. Zakeri, M.H. Moayed, A. Davoodi, H. Eshghi, *Corros. Sci.* 53 (2011) 3058.
72. R. Solmaz, G. Kardas, M. Culha, B. Yazici, M. Erbil, *Electrochim. Acta.* 53 (2008) 5941.
73. Xianghong Li, Shuduan Deng, Hui Fu, Guannan Mu, *Corros. Sci.* 52 (2010) 1167.
74. Xianghong Li, Shuduan Deng, Hui Fu, Guannan Mu, *Corros. Sci.* 51 (2009) 620.
75. L. Afrine, A. Zarrouk, H. Zarrok, R. Salghi, R. Tourir, B. Hammouti, H. Oudda, M. Assouag, H. Hannache, M. El Harti, M. Bouachrine, *J. Chem. Pharm. Res.* 5 (2013) 1474.
76. Sh. Pournazari, M.H. Moayed, M. Rahimizadeh, *Corros. Sci.* 71 (2013) 20.
77. K. G. Zhang, B. Xu, W. Z. Yang, *Corros. Sci.* 90 (2015) 284.
78. F. E. Hajjaji, B. Zerga, M. Sfaira, M. Taleb, M. Ebn Touhami, B. Hammouti, S.S. A. Deyab, H. Benzeid, El M. Essassi, *J. Mater. Environ. Sci.* 5 (1) (2014) 255.
79. K.R. Ansari, M.A. Quraishi, *Journal of the Taiwan Institute of Chemical Engineers.* 54 (2015) 145.

80. M. Gopiraman, P. Sakunthala, D. Kesavan, V. Alexramani, I. S. Kim, N. Sulochana, *J. Coat. Technol. Res.* 9 (2012) 15.
81. D. A. López, W. H. Schreiner, S. R. de Sánchez, S. N. Simison, *Appl. Surf. Sci.* 207 (2003) 69.
82. S. T. Keera, *J. Sci. Ind. Res.* 62 (2003) 188.
83. H. Ma, S. Chen, Z. Liu, Y. Sun, *J. Mol. Struct. (Theochem)*. 774 (2006) 19.
84. A. Ehsani, M. G. Mahjani, R. Moshrefi, H. Mostanzadeh, J.S. Shayeh, *RSC adv.* 4(38) (2014) 20031.
85. S. Kr. Saha, P. Ghosh, A. R. Chowdhury, P. Samanta, N. C. Murmu, A. K. Lohar, P. Banerjee, *Can. Chem. Trans.* 2 (2014) 381.
86. G. Gao, C. Liang, *Electrochim. Acta.* 52 (2007) 4554.
87. A. Yurt, S. Ulutas, H. Dal, *Appl. Surf. Sci.* 253 (2006) 919.
88. N.K. Allam, *Appl. Surf. Sci.* 253 (2007) 4570.
89. H. Ju, Z. P. Kai, and Y. Li, *Corros. Sci.* 50 (2008) 865.
90. J. Zhang, G. Qiao, S. Hu, Y. Yan, Z. Ren, L. Yu, *Corros. Sci.* 53 (2011) 147.
91. V.S. Sastri, *Principles and Application, John Wiley and Sons*, (1998).
92. T. Koopmans, *Physica.* 1 (1933) 104.
93. R.G. Pearson, *J. Org. Chem.* 54 (1989) 1423.
94. R.G. Parr, L. Szentpaly, S. Liu S, *J. Am. Chem. Soc.* 121 (1999) 1922.
95. P. Udhayakala, T. V. Rajendiran, S. Gunasekaran, *Journal of Chemical, Biological and Physical Sciences A*, 2 (2012) 1151.
96. F. Bentiss, M. Traisnel, M. Lagrenee, *J. Appl. Electrochem.* 31(2001) 41.
97. I. Lukovits, E. Kálmán, *Corrosion.* 57 (2001) 3.
98. I. B. Obot, Z. M. Gasem, *Corros. Sci.* 83 (2014) 359.
99. E.E. Ebenso, D.A. Isabirye, N.O. Eddy, *Int. J. Mol. Sci.* 11 (2010) 2473.
100. N.O. Obi-Egbedi, K.E. Essien, I.B. Obot, E.E. Ebenso, *Int. J. Electrochem. Sci.* 6 (2011) 913.
101. S. Chen, T. Kar, *Int. J. Electrochem. Sci.* 7 (2012) 6265.
102. J. N. Asegbeloyin, P. I M. Ejikeme, L. O. Olasunkanmi, A. S. Adekunle, E. E. Ebenso, *Materials.* 8 (2015) 2918.
103. M.A. Amin, M.A. Ahmed, H.A. Arida, F. Kandemirli, M. Saracoglu, T. Arslan, M.A. Basaran, *Corros. Sci.* 53 (2011) 1895.
104. A. U. Ezeoke, O.G. Adeyemi, O.A. Akerele, N.O. Obi-Egbedi, *Int. J. Electrochem. Sci.* 7 (2012) 534.
105. R.G. Parr, W. Yang, *J. Am. Chem. Soc.* 106 (1984) 4049.
106. S. Kaya, B. Tüzün, C. Kaya, I. B. Obot, *Journal of the Taiwan Institute of Chemical Engineers.* 58 (2016) 528.
107. M. A. Hegazy, A. M. Badawi, S. S. A. E. Rehim, W. M. Kamel, *Corros. Sci.* 69 (2013) 110.
108. H. Jafari, I. Danaee, H. Eskandari, M. RashvandAvei, *J. Mater. Sci. Technol.* 30(2014) 239.
109. A. Liu, X. Ren, J. Zhang, C. Wang, P. Yang, J. Zhang, M. An, D. Higgins, Q. Li, G. Wu, *RSC Adv.* 4 (2014) 40606.
110. M. Sahin, G. Gece, F. Karci, S. Bilgic, *J Appl Electrochem.* 38 (6) (2008) 809.